SUPPLEMENTARY INFORMATION

An outer membrane channel protein of *Mycobacterium tuberculosis* with exotoxin activity

Olga Danilchanka[1], Jim Sun[1], Mikhail Pavlenok[1], Christian Maueröder[2], Alexander Speer[1], Axel Siroy[1], Joeli Marrero[3], Carolina Trujillo[3], David L. Mayhew[4], Kathryn Doornbos[1], Luis E. Muñoz[5], Martin Herrmann[5], Sabine Ehrt[3], Christian Berens[2] and Michael Niederweis[1]*

[1] Department of Microbiology, University of Alabama at Birmingham, Birmingham, AL, USA
[2] Department of Biology, Friedrich-Alexander-Universität Erlangen-Nürnberg, Erlangen, Germany
[3] Department of Microbiology and Immunology, Weill Cornell Medical College, New York, NY, USA
[4] Department of Radiation Oncology, University of Alabama at Birmingham, Birmingham, AL, USA
[5] Department of Internal Medicine - Rheumatology and Immunology, Friedrich-Alexander-Universität Erlangen-Nürnberg, Erlangen, Germany

*** Corresponding author:**

Dr. Michael Niederweis

University of Alabama at Birmingham

Department of Microbiology, BBRB 609

845 19th Street South, Birmingham, AL35294, U.S.A.

Phone: +1-205-~~996-2711~~

E-Mail: mnieder@uab.edu

MATERIALS AND METHODS

Chemicals, enzymes, bacterial strains, media and growth conditions. Hygromycin B was purchased from Calbiochem. All other chemicals were purchased from Merck or Sigma at the highest purity available. Enzymes for DNA restriction and modification were from New England Biolabs and Invitrogen. Oligonucleotides were obtained from IDT. Doxycycline was purchased from Sigma and dissolved in Millipore-filtered water prior to use. *E. coli* DH5α was used for cloning experiments and was routinely grown in Luria-Bertani broth at 37°C. *M. smegmatis* strains were grown at 37°C in Middlebrook 7H9 medium (Difco) supplemented with 0.2% glycerol and 0.01% Tyloxapol or on Middlebrook 7H10 plates supplemented with 0.5% glycerol. *M. bovis* BCG (Strain Institute Pasteur) and *M. tuberculosis* H37Rv were grown in Middlebrook 7H9 medium (Difco) supplemented with 0.2% glycerol, 0.02% Tyloxapol and 10% OADC (Remel) or on Middlebrook 7H10 plates supplemented with 0.5% glycerol and 10% OADC (Remel). For the avirulent, auxotrophic *M. tuberculosis* $mc^2$6206 strains, media included 24 µg/ml pantothenate and 50 µg/ml L-leucine as supplements (1). Antibiotics were used when required at the following concentrations: hygromycin (200 µg/ml for *E. coli*, 50 µg/ml for mycobacteria), kanamycin (30 µg/ml). Hartmans-de Bont (HdB) medium supplemented with 0.01% Tyloxapol and the appropriate carbon source was used as a minimal medium for growth experiments for *M. bovis* BCG (2). As *Mtb* grows poorly in HdB medium, standard 7H9 medium supplemented with 0.01% Tyloxapol (without OADC) and a specified carbon source were used for growth experiments with H37Rv.

Construction of plasmids. Plasmids and oligonucleotides used in this study are listed in tables S1 and S2, respectively. To construct a new integrative vector without a *bla* expression cassette and with low copy number in *E. coli,* plasmid pML113 (3) was digested with SspI and ClaI followed by T4 DNA polymerase treatment to generate blunt double-stranded DNA. A new pBR322 origin of replication was cloned in from pET21a(+) *(*Novagen*,* WI) digested with FspI and DraI. In order to be able to use a PacI restriction site in subsequent construction steps, the obtained plasmid was digested with PacI, followed by a blunt-end reaction using T4 DNA polymerase and re-ligation resulting in pML2008. An *mspA* expression cassette under control of p_{imyc} was obtained from pMN013 (4) by digestion with ClaI followed by a fill-in reaction with T4 DNA polymerase and digestion with SpeI. The obtained fragment was cloned into pML2008 digested with SpeI and PmeI resulting in pML2009. The *cpnT* gene was amplified by PCR from genomic DNA of H37Rv (obtained from the Colorado State University as part of the National Institutes of Health (NIAID) contract HHSN266200400091C entitled "Tuberculosis Vaccine Testing and Research Materials") using the oligonucleotides CN2542 and CN1394 which introduced a PacI restriction site at the 5'-end and a HindIII restriction site at the 3'-end. The obtained PCR fragment and pML2009 were digested with PacI and HindIII and ligated to yield the plasmid pML2228. An integrative *cpnT* complementation vector was obtained by amplification of the *cpnT* gene from genomic DNA of *Mtb* H37Rv with oligonucleotides CN1537 and CN1397 which introduced the PacI restriction site at the 5'-end and HindIII restriction site at the 3'-end. The obtained PCR fragment and the plasmid pML2009 were digested with PacI and HindIII and were ligated resulting in pML2010. To obtain the complementation vector pML2046 encoding the N-terminal domain of CpnT (aa 1-448), PCR amplification was done from genomic DNA using the oligonucleotides CN1537 and CN1729, followed by digestion with PacI and HindIII and ligation with pML2009 digested with the same enzymes. To obtain a tagged version of *cpnT*, a two-step PCR amplification was employed: A His-tag was added by using CN1393 (introduction of a NdeI site on the 5' end) and CN1824, an HA-tag was added by using CN1393 and CN1825 (introduction of a HindIII site on the 3' end and an EcoRV site between *cpnT* and the HA-tag). The obtained PCR fragment was digested with NdeI and HindIII and ligated into pNIT-1::*gfp* (5) digested with the same enzymes resulting in pML2024. To exchange the resistance cassette, pML2024 was digested with HpaI and XbaI and ligated into pMS2 (6) digested with EcoRV and XbaI to obtain pML2031. To create the integrative vector pML2023 containing a His-HA-tagged version of full length *cpnT*, the gene was amplified with CN1537 and CN1718 using pML2024 as a template. The obtained PCR fragment was digested with PacI and HindIII and ligated into pML2009 digested with the same enzymes.

The nitrile-inducible vector pML2040 encoding the N-terminal domain of CpnT and a His-HA tag was obtained by PCR amplification of *cpnT* using CN1393 and CN1720. This PCR fragment and DNA of pML2031 were digested with NdeI and EcoRV and ligated to obtain the vector pML2040. The vector pML2172 containing the nitrile-inducible $cpnT_{G818V}$ gene was obtained by PCR amplification of *cpnT* from pML2031 using primers CN1390 and CN1644. The G818V point mutation in full length *cpnT* was introduced using the overlapping primers CN5012 and CN5013. The obtained PCR fragments were digested with EcoRV and NsiI and cloned into pML2031 digested with same enzymes.

In order to obtain a nitrile-inducible *cpnT-gfp* fusion the plasmid pML2025 was constructed employing overlap PCR: *cpnT* was amplified with the primers CN1393 and CN1824 using pML2024 as a template, *gfp* was amplified from pML515 with the primers CN5010 and CN5011. The fragments contained overlapping sequences and served as

template in a PCR amplification with the primers CN1393 and CN5010 that yielded the fusion of *cpnT* and *gfp*. The PCR fragment obtained was digested with PacI and HindIII and cloned into pML2040 digested with the same enzymes. To obtain the *E. coli* expression vector pML2123 encoding a $cpnT_{aa650\text{-}847}$-*gfp* fusion, PCR amplification was done with the primers CN1644 and CN1982 using pML2025 as a template. The obtained PCR fragment was cloned into pMN016 digested with the same enzymes.

The vector pML2009 served as a parent vector to construct the vectors pML2084, pML2087 and was digested with PacI and HindIII. Corresponding PCR fragments were amplified from genomic DNA and digested with PacI and HindIII. To construct the vector pML2084 containing an *esxEF-rv3902c* transcriptional fusion, the *esxFE* region was amplified with the primers CN2932 and CN2935. *rv3902c* was amplified with the primers CN2934 and CN1584. Overlap PCR was done to create the *esxFE-rv3902c* fusion with primers CN2932 and CN1584. To construct the vector pML2087, *rv3902c* was amplified with CN1584 and CN1585. To construct the replicative vector pML2904 containing a $cpnT_{NTD\text{-}HA\text{-}His}$- *esxFE -rv3902c* fusion, pML2084 was used as a template for PCR amplification of *esxFE-rv3902c* with the primers CN2932 and CN2933. The obtained PCR fragment was digested with PacI and AseI, followed by a fill-in reaction using T4 DNA polymerase, and ligated into pML2040. pML2040 was digested with PacI, followed by a fill-in reaction with T4 DNA polymerase. To obtain a parental knock-out vector in which upstream and downstream cassettes can be conveniently exchanged, pML515 was digested with (i) NotI and BamHI (large fragment), and (ii) BamHI and SpeI (small fragment). Both fragments were blunt-ended with T4 DNA polymerase and re-ligated back to remove the SpeI cloning sites. The obtained vector was consecutively digested with SpeI/SwaI and with PacI/NsiI to clone upstream and downstream regions of *cpnT*, respectively. The knockout vector pML1113 was constructed by amplification of the *cpnT* upstream region with CN1396 and CN1398, and its downstream region with CN1397 and CN1399. The upstream region was digested with SpeI and SwaI and the downstream region was digested with PacI and NsiI.

To construct a eukaryotic expression vector for *cpnT*, the gene was codon-optimized using Optimizer (http://genomes.urv.es/OPTIMIZER/). Optimization of the *cpnT* gene for expression in *E. coli* was done using *E. coli* K12 codon usage data and a guided random method of optimization and synthesis by GenScript (Piscataway, NJ). Using the synthesized gene as a template, PCR amplification was done for $cpnT_{CTD}$ (aa 650-847) with primers CN1904 and CN1807-1907. The PCR fragment was cloned into the parent vector pRK7 using SalI and EcoRI resulting in the plasmid pML2093. To obtain a non-toxic mutant of $cpnT_{CTD}$, site-directed mutagenesis using the combined chain reaction (CCR) was performed with flanking primers CN1904 and CN1807-1907 and the primer CN1994 that introduced a G818V point mutation in $cpnT_{CTD}$. The CCR fragment was digested with SalI/EcoRI and ligated into pRK7 digested with the same enzymes to obtain plasmid pML2138. To construct the Tet-inducible $cpnT_{CTD}$-expressing vector pWHE655-$CpnT_{CTD}$, a DNA fragment encoding $CpnT_{CTD}$ (aa 651 – 846) was amplified with the primers D3fwd-nsUEcoRI and D3rev-shEcoRV using pML2093 as a template. The PCR product was digested with EcoRI and EcoRV and ligated with likewise-restricted pWHE655-revCasp-3.

In order to complement the *M. tuberculosis cpnT* mutant for macrophage infection experiments, we expressed the entire operon *esxF-rv3902c* under control of the strong constitutive promoter p_{imyc} and integrated the construct in the chromosome at the L5 site. The operon was amplified by PCR from genomic DNA using the primer pair CN1584 and CN3042. The obtained PCR fragment was digested with PacI and HindIII and ligated into pML2087 digested with the same enzymes resulting in pML3009. As a control and to determine that the observed toxicity is caused by $CpnT_{CTD}$, we truncated *cpnT* by replacing $cpnT_{CTD}$ with a HA-His tag while leaving the operon organization intact. The gene $cpnT_{NTD}$-HA-His was amplified from the plasmid pML2040 using primers CN1390 and CN3047. A second fragment encoding the downstream gene *rv3902c* was amplified from genomic DNA using the primer pair CN3048 and CN1584. The obtained fragments were fused by overlap PCR using the primers CN1390 and CN1584. After digestion with NheI and HindIII, the fragment was ligated into similarly digested pML3009 to yield the plasmid pML3107.

For production of antibodies against $CpnT_{CTD}$, the recombinant non-toxic domain (mutant domain G818V) was produced in *E. coli*. The expression vector was derived from the plasmid pMAL-c5X (New England Biolabs). To enable a two-step affinity purification of $CpnT_{CTD,}$ an N-terminal hexa-histidine encoding sequence was added to the *malE* gene from the pMAL-c5X vector, by two-step PCR using the primers CN2239 and CN2240 paired with the primer CN2241. The resulting fragment was digested with the enzymes MfeI and BglII and was ligated with the similarly digested plasmid pMAL-c5X, yielding the plasmid pML1925. Subsequently, the C-terminal recognition sequence for the protease Xa was exchanged for the recognition sequence of the protease NIa: the oligonucleotides CN2811 and CN2812 were phosphorylated using the T4 polynucleotide kinase prior to their hybridization, yielding a DNA fragment encoding the poly-asparagine linker and the Tobacco Etch Virus (TEV) protease NIa recognition sequence, flanked by SacI and NdeI cohesive ends. This fragment was ligated with the vector pML1925 digested with the same restriction enzymes, yielding the plasmid pML1947. Lastly, the sequence encoding for the non-toxic domain $_{G818V}CpnT_{651\text{-}846}$ was

amplified by PCR from the plasmid pML2123, using the primers CN1922 and CN2817. The resulting fragment was digested by NdeI and HindIII and ligated with the similarly digested plasmid pML1947, yielding the expression vector pML1950 encoding for the 6xHis-MalE-polyAsp-TEV-$_{G818V}$CpnT$_{651-846}$ polypeptide chain.

Construction of *cpnT* deletion mutant in *M. tuberculosis*. *Mtb* H37Rv cells were transformed with the *cpnT* deletion vector pML1113, which carries approximately 1 kb of the upstream and downstream regions of *cpnT*, and the reporter genes *gfp*$_m^{2+}$ and *xylE*. After 21 days at 37°C, fluorescent colonies that also turned yellow in the presence of 1% catechol were picked and transferred in 10 ml of Middlebrook 7H9 broth supplemented with hygromycin and OADC. The culture was grown at 37°C to an OD_{600} exceeding 1.0. Then, 100 µl were plated on Middlebrook 7H10 medium containing OADC and hygromycin, and incubated at 40°C to select for bacteria in which the plasmid was integrated by homologous recombination. A colony that tested positive for both reporters was picked and grown in Middlebrook 7H9/OADC/hygromycin broth. Appropriate volumes of the culture with an OD_{600} exceeding 1.0 were plated on Middlebrook 7H10/OADC/hygromycin medium supplemented with 2% sucrose to select for double crossover events (ML832). The loss of *xylE* expression indicated the excision of the plasmid backbone leaving the *loxP- gfp*$_m^{2+}$*-hyg-loxP* cassette. After 30 days at 37°C, four fluorescent colonies without XylE activity were picked and transferred into Middlebrook 7H9/hygromycin. One candidate was picked and competent cells were transformed with pCreSacB1 to excise the *loxP- gfp*$_m^{2+}$*-hyg-loxP* cassette. One colony was picked and grown in Middlebrook 7H9/kanamycin. Appropriate dilutions were plated on Middlebrook 7H10 medium supplemented with 2% sucrose and incubated at 37°C. After 21 days four non-fluorescent colonies were picked and grown in Middlebrook 7H9 broth. After the culture reached an OD_{600} of approximately 1, 5 µl of the culture were dropped on Middlebrook 7H10 plates containing either kanamycin, hygromycin or no antibiotics. All colonies were sensitive to both antibiotics indicating that the *hyg* cassette had been efficiently excised and pCreSacB1 was lost. The unmarked *Mtb cpnT* mutant ML1552 as well as *Mtb* ML832 were confirmed by Southern blot analysis. Presence of phthiocerol dimycocerosates (PDIMs) that are essential for *Mtb* infection and can be spontaneously lost during mutant construction (7) was confirmed using a previously published protocol (8). The *Mtb cpnT* mutant ML1552 was transformed with empty integration plasmid pML2008 and the integrative expression plasmids for *cpnT*$_{NTD}$ (pML2046) and full-length *cpnT* (pML2228) resulting in the *Mtb* strains ML1504, ML1518 and ML1543 respectively. The strain *Mtb* ML812 containing the empty integrative vector pML2008 was used as a control in the growth experiments.

Glycerol uptake experiments. Glycerol uptake experiments were carried out as described previously (9) with modifications. Cells of the *M. bovis* BCG strains ML383, ML386, ML387 and ML387 were harvested from liquid cultures at an OD_{600} of 0.5-1.0 by centrifugation, washed twice in uptake buffer (50 mM Tris pH 6.9, 15 mM KCl, 10 mM $(NH_4)_2SO_4$, 1 mM $MgSO_4$, 0.02% Tyloxapol), and resuspended in the same buffer (mean dry weight is 0.5-1 mg/ml). Cells were pre-incubated at 37°C for 15 min before addition of [^{14}C] glycerol (specific activity: 146 mCi/mmol). The final concentration of radioactively-labeled glycerol was 3 µM. The experiments were performed twice in triplicate.

Subcellular fractionation experiments. The subcellular fractionation experiments were carried out as described previously with modifications (10). *M. smegmatis* mc^{2}155 containing the plasmids pML2040 (expression of *cpnT*$_{NTD}$) or pML2172 (expression of full length *cpnT* encoding the non-toxic CpnT G818V mutant). Cells in early log phase cultures were induced with with 1 µM isovaleronitrile in DMSO for 3 h before the cells were harvested. After fractionation by ultracentrifugation (10) samples were analyzed by gel electrophoresis and immunoblotting. CpnT was detected with an antibody (Sigma) that recognizes the human influenza hemagglutinin (HA)-tag at the C-terminus of CpnT. Polyclonal antibodies against IdeR and MspA were used as controls.
Subcellular fractionation of *Mtb* mc^{2}6206 was done as described above. Proteins were detected using the rabbit antiserum raised against IdeR, MctB and CpnT C-terminal domain. Horseradish peroxidase-coupled secondary anti-mouse or anti-rabbit antibodies from goats (Sigma) were used. Blots were developed using ECL Western blotting substrate (Pierce). LabWorks (UVP) chemoluminescence imaging system and software were used to visualize the luminescence.

Surface detection of proteins in *M. tuberculosis* by flow cytometry.
Δ*cpnT Mtb* mc^{2}6206 mutant ML2004 and a CpnT$_{HA}$-overexperession strain ML2010 containing pML2031 plasmid were used for CpnT expression analysis. Expression of *cpnT* under the control of a p_{NIT} promoter was induced for 48 h. MspA was expressed in *Mtb* mc^{2}6206 using pMN016 plasmid. MbtG$_{HA}$ was expressed in *Mtb* mc^{2}6230 using pML1828 plasmid. Bacteria from mid-log phase cultures were fixed with 4% paraformaldehyde for 30 min at room temperature. To detect the HA–tag of MbtG and CpnT a rabbit anti-HA antibody (Sigma) were used. For detection of MspA we used a mouse anti-MspA monoclonal antibody. The primary antibodies were used at a 1:50 dilution in PBS + 0.05% Tween

80 to stain the bacterial surface for 30 min. Following three washes, bacteria were stained with anti-rabbit AlexaFluor 488 or anti-mouse-FITC antibodies at a dilution of 1:500 for 30 min. Bacteria were washed three times and fluorescence was quantified by flow cytometry. Surface accessible CpnT, MbtG and MspA was quantified by flow cytometry and displayed as histograms.

Purification of the N-terminal domain of CpnT. Purification of $CpnT_{NTD}$ was done from *M. smegmatis* ML1910 carrying plasmid pML2904. ML1910 is an Msp-porin-free mutant, in which the His-tag binding part of GroEL was disrupted by insertion of a *bxb1* phage (11). ML1910/pML2904 was grown in 7H9/0.5% glycerol/0.5% glucose/0.5% Tween-80/0.5 g/L BSA. Cells were grown until an OD_{600} of 0.2 was reached. 5 µM isovaleronitrile was added to induce gene expression. After 48 h of growth, cultures were harvested by centrifugation and washed twice with PBS (140 mM NaCl, 2 mM KCl, 10 mM K_2HPO_4/KH_2PO_4 pH 7.4) containing 1 mM phenylmethanesulfonyl fluoride (PMSF) and 1 mM ethylenediaminetetraacetic acid (EDTA). Cell were resuspended and lysed by sonication (15 min, 12 Watt output power). Afterwards, a pellet was obtained by centrifugation at 4,000 x g and was treated with 1 mg/ml of lysozyme and 0.01 mg/ml of DNaseI for 2 hours at 37°C. The sonication and centrifugation step was performed again as described above. The pellet contained the majority of the N-terminal domain of CpnT and, therefore, was used for further purification steps. Proteins were extracted from the pellet with PBS/0.8% sodium dodecyl sulfate (SDS) overnight at room temperature. Non-soluble material was removed by centrifugation at 16,000 x g for 10 min at room temperature. Extracted proteins were purified using Ni-NTA resin (Quagen) following manufacturer recommendations. Elution was done with 250 mM imidazole. Protein fractions containing $CpnT_{NTD}$ were pooled together and dialyzed against AOPO5 buffer (25 mM HEPES, 10 mM NaCl, 0.5% *n*-octylpolyoxyethylene (*n*-octyl-POE), pH 7.5). Anion-exchange purification was done next using HiTrap Q FF (GE Healthcare) as described elsewhere (12). Elution was done using a salt concentration gradient ranging from 0.01 M to 2 M NaCl. To isolate $CpnT_{NTD}$ from the gel, protein purified by anion-exchange chromatography was concentrated using Amicon tubes (Millipore) with a 10 kDa molecular weight cut-off. The retentate was loaded onto a 10% SDS-polyacrylamide gel and stained with Simple Blue Safe Stain (Invitrogen). Note that the $CpnT_{NTD}$ protein sample was mixed with a β-mercaptoethanol-free loading buffer and the mixture was not boiled prior to loading on the gel to preserve disulfide bridges. Bands corresponding to different oligomeric forms of $CpnT_{NTD}$ were cut from the gel with a razor. Next, gel pieces were crushed and incubated in elution buffer (50 mM Tris-HCl, 150 mM NaCl, 0.1 mM EDTA, 0.5% n-octyl-POE, pH 7.5) overnight at room temperature. Spin-X centrifuge tube filters (Costar) were used to remove gel pieces from the sample by centrifuging at 100 rpm for 1 minute at room temperature. Next, samples were concentrated using Microcon centrifugal filters (Millipore) with a 10 kDa molecular weight cut-off. Recovered protein was either used for bilayer experiments or stored at 4°C. For bilayer experiments samples were treated with BioBeads SM-2 at 40 mg/ml concentration to remove detergent from solution. As a control, we used a “protein-free” SDS-polyacrylamide gel. A gel piece of the same size as in the protein containing sample was cut from the gel and was subjected to all gel extraction procedures as described above.

Protein analysis. All samples were mixed with protein loading buffer (160 mM Tris-Cl pH 7.0, 12% SDS, 32% glycerol, 0.4% Bromophenol blue), boiled when required for 10 min and separated using a 10% SDS- polyacrylamide gel. The protein gel was blotted overnight at 50 mA in transfer buffer (25 mM Tris base, 192 mM Glycine, 0.1% SDS, 20% methanol) onto a polyvinylidenedifluoride (PVDF) membrane. $CpnT_{NTD}$ was detected with anti-HA-HRP antibody (Sigma) using the ECL plus kit (Amersham). A LabWorks (UVP) chemoluminescence imaging system and software were used to visualize and quantify the luminescence.

Formation of giant unilamellar vesicles (GUVs). To obtain planar lipid bilayers, GUVs were prepared by the electroformation method (13) using indium tin oxide (ITO)-coated glass slides as previously described (14, 15). Two ITO-coated glass slides serve as electrodes in a Nanion Vesicle Prep Pro setup (Nanion Technologies GmbH, Munich, Germany). 20 µl of lipid mixture (10 mM 1,2-diphytanoyl-sn-glycero-phosphatidylcholine (DphPC), 1 mM cholesterol in chloroform) were deposited on the electro conductive side of the ITO slide. After complete evaporation of the solvent, 280 µl of 1 M sorbitol solution was added onto the lipid film contained within an O-ring. Then, an ITO-coated slide was placed on top of the O-ring so that two ITO-coated sides face each other. Electroformation of GUVs was controlled by a Nanion Vesicle Prep Pro setup using the built-in basic protocol. In particular, an alternating voltage of 3 V peak to peak was applied with a progressive increase for the rise time and a decrease for the fall time to avoid abrupt changes, which might break GUVs otherwise. The alternating current was applied to the ITO-slides over a period of 2 h at a frequency of 5 Hz at 36°C. After swelling, GUVs were either used directly for downstream applications or stored at 4°C.

Reconstitution of $CpnT_{NTD}$ in giant unilamellar vesicles (GUVs). After purification of $CpnT_{NTD}$, a protein sample in solution containing 0.5% octyl-POE was mixed with 200 µl of GUVs to give a final protein concentration of

approximately 0.3 µg/ml. The mixture was incubated at room temperature for 1 hour to facilitate protein reconstitution into vesicles. Next, BioBeads® SM-2 were added at a concentration of 40 mg/ml to remove detergents from the solution and the mixture was incubated at 4°C overnight. Upon centrifugation at 100 rpm at 20°C for 1 min supernatant which contained proteoliposomes of $CpnT_{NTD}$ was used directly for electrophysiological experiments or stored at 4°C.

Planar lipid bilayer formation. Port-o-Patch system utilizes NPC-1® borosilicate glass chips to obtain planar lipid bilayer. NPC-1® has an aperture of approximately 1 micron in diameter. When a GUV contacts the glass surface of the chip, the vesicle bursts and forms a planar lipid bilayer with a seal resistance ranging from one to hundreds of GΩ (14, 16). To obtain planar lipid bilayers 5-10 µl of either GUVs or proteoliposomes were added onto the chip. A negative pressure of -30 mbar was applied to position the GUV or the proteoliposomes onto the glass aperture and was kept during recordings to help maintain the lipid bilayer. Lipid bilayers formed within several seconds after addition of the vesicles with a frequency of approximately 80%. Seal resistance ranged from 1 to >100 GΩ. However, when proteoliposomes were used the frequency of bilayer formation was reduced to 20%. This may be attributed to the presence of detergents in the protein sample and proteoliposome formation. Similar observations of reduced bilayer formation with proteoliposomes were described in OmpF studies using the same planar patch clamp set-up (14). The bilayer formation process was computer-controlled by the PatchControl software (Nanion).

Measurements of channel activity of $CpnT_{NTD}$. Bilayer experiments were performed with the Port-a-Patch automated patch clamp system (Nanion Technologies GmbH, Munich, Germany). Based on the aperture diameter (1 micron) of the chip and a specific capacitance of DPhPC of 0.5 µF/cm (16), the membrane capacitance was estimated to be in the order of a few fF. Experiments were done in symmetric solutions of 1 M KCl, 10 mM HEPES, pH 6.0. EPC-9 patch clamp amplifier (HEKA Electronics, Germany) was used to amplify the current from a Port-a-Patch system equipped with Ag/AgCl electrodes. Data were recorded and digitized by Patchmaster software from HEKA. The signal was filtered at 10 kHz (Bessel filter, HEKA amplifier) and digitized at a sampling rate of 50 kHz. IGOR Pro 5.03 (WaveMetrics) software was used for analysis and graph preparation. Two sets of experiments were performed to measure channel-forming properties of $CpnT_{NTD}$. First, we used proteoliposomes containing purified $CpnT_{NTD}$. Second, different oligomeric forms of $CpnT_{NTD}$ with electrophoretic mobilities of 56 kDa, 130 kDa and 200 kDa were excised from a gel and analyzed. 5-10 µl of proteoliposomes were used to obtain a bilayer. For the oligomers characterization, a stable membrane was obtained first. After seal formation, protein oligomers (concentration of approximately 0.3 µg/ml) were manually added on top of the NPC-1 chip. Control experiments were performed by using protein-free GUVs or GUVs made in the presence of extracts from “protein-free” parts of the SDS-polyacrylamide gel.

Analysis of average single-channel conductance of $CpnT_{NTD}$. After addition of protein to the lipid bilayer setup a step-wise current increase of the membrane was observed. This increase is indicative of a single channel insertion or opening in the lipid bilayer. We then measured the current of each individual step recorded in a multi-channel experiment. Then, a histogram of the distribution of all current values (all data points) was generated from the current traces of multi-channel recordings. Each peak in the histogram represents an average current value for a corresponding insertion/opening event. Averaged values were carefully inspected and adjusted if necessary in order to include values of fast events into the resulting single-channel analysis. A total of 50 single-channels of the 200 kDa oligomeric form of $CpnT_{NTD}$ were identified and plotted as distribution histogram (Fig. 3D). The IgorPro software (WaveMetrics) was used to generate the histograms and to fit the data to a Gaussian distribution. In addition, IgorPro was used for trace representation following the export of a trace from PatchMaster into IgorPro compatible file format. The resulting distribution histogram was generated using SigmaPlot.

Analysis of secondary structure of CpnT. Analysis was done as described previously (17).

Identification of non-toxic mutants of $CpnT_{CTD}$ in *E. coli*. Mycobacterial shuttle vectors containing transcriptional fusions of the p_{smyc} promoter and the wt *cpnT*$_{CTD}$ gene were toxic in *E. coli*, probably due to low level background. Using such a vector, only clones containing mutated $CpnT_{CTD}$ were obtained. To distinguish in-frame point mutations from frame-shift or nonsense mutations, we developed a reporter system that consists of a translational fusion *of cpnT*$_{CTD}$ and *gfp* under the control of the mycobacterial promoter p_{smyc}. A *cpnT*$_{CTD}$-*gfp* fusion was amplified from pML2025 which contains a *cpnT-gfp* fusion under control of the silent p_{NIT} promoter, digested and cloned into pMN016 containing p_{smyc}. Under such conditions only clones containing point mutations in *cpnT*$_{CTD}$ that inactivate toxicity of the protein will be viable and fluorescent. Clones containing wild-type protein will not be viable, and clones containing stop mutations, frame-shift mutation, or mutations in other relevant sequences such as the p_{smyc} promoter, the Shine-Dalgarno sequence or the origin of replication will not be *gfp*-positive, and are excluded from further analysis. Using this approach three point mutations that attenuate toxicity in *E. coli* were identified (G752V, G811E and G818V).

Production of recombinant $_{G818V}$CpnT$_{651-846}$. The expression vector pML1950 was transformed into *E. coli* C43 (DE3) cells and cells were grown in baffled flasks at 37ºC, 200 rpm with LB medium supplemented with 0.3% (m/v) glucose and 150 µg/mL carbenicillin. Once the OD_{600} reached ~0.8, the cells were induced with 0.6 mM isopropyl β-D-1-thiogalactopyranoside (IPTG) and grown in the same conditions until they reached a plateau phase (OD_{600} ~4.5) for about 3 hours. The cells were harvested by centrifugation (8,000 x g, 4ºC, 10 minutes). The pellets were washed with ice cold TNG buffer (50 mM Tris pH 7.5, 300 mM NaCl, 10% (v/v) glycerol) and resuspended in ice-cold TNG buffer (7 mL per g of wet pellet) supplemented with 2 mM Tris(2-carboxyethyl)phosphine hydrochloride (TCEP, Soltec Ventures), 1 mM PMSF, 1 mM EDTA, 2.5 units benzonase/mL, 1 mg/mL lysozyme. The cells were lyzed by sonication (Misonix, on ice, 5 seconds bursts, 6 W output, total sonication time of 1 min/mL suspension), incubated on ice for 30 minutes and sonicated a second time. The lysed cells were spun down (10,000 x g, 30 minutes, 4ºC) to remove debris and the supernatant was applied to the same volume of Talon resin (Clontech), equilibrated in TNG buffer supplemented with 1 mM TCEP, 1 mM PMSF. After gentle shaking for 2 hours at 4ºC, the resin was allowed to settle in the column, the flow-through was recovered and the resin was washed with the same buffer (10 bed volumes). Elution of the bound proteins was carried out by passing the same buffer containing 150 mM imidazole in ½ bed volume fractions. The fractions containing the fusion protein 6xHis-MalE-polyAsp-NIa-$_{G818V}$CpnT$_{651-846}$ were pooled and dialyzed against TNG buffer, 1 mM TCEP to remove excess imidazole. Recombinant TEV protease NIa mutant S219V (18) was added and the digestion carried on for 72 hours at 4ºC. Subsequently, the maltose binding protein was removed by capturing it on an amylose column equilibrated in the same buffer. The protein content was monitored by following the absorption of the samples at 280 nm. The fractions containing protein (flow-through and first wash) were recovered, pooled, diluted six-fold with 50 mM Tris pH 7.0, 10% glycerol buffer to reach an NaCl concentration of 50 mM and further separation was achieved by anion exchange on a HiTrap Q FF cartridge (GE Healthcare Life Sciences) using a 10-500 mM NaCl gradient. The fractions of the main elution peak centered around 300 mM NaCl were pooled and submitted to preparative size exclusion chromatography on a 16/60 Superdex 75pg column (GE Healthcare Life Sciences) equilibrated and operated with 20 mM Tris pH 8, 200 mM NaCl, at a flow rate of 1 mL/min. The fractions containing $_{G818V}$CpnT$_{651-846}$ were pooled and concentrated with an Amicon (10 kDa cut off) to a final concentration of 1 mg/mL, and 1 mM TCEP, 1 mM EDTA, 1 mM PMSF were added as preservatives. This protocol yielded 5 to 10 mg of $_{G818V}$CpnT$_{651-846}$ per liter of culture, ≥ 95% pure as determined by SDS-PAGE analysis.

Production of antibodies against CpnT and culture filtrate of *Mtb*. Recombinant non-toxic CpnT$_{CTDG818V}$ (aa651-846) protein was used for the production of polyclonal antibodies in rabbits (Open Biosystems). Briefly, two animals were immunized twice with a 35 days interval (days 5 and 40). Polyclonal antibodies were generated by immunization with SDS-PAGE-purified protein in adjuvant Titermax. On day 56, the animals were bled, and the antisera were tested by Western blot analysis. The antiserum of the animal PA4158 was judged of adequate quality, yielding a high signal/noise ratio. The animals were bled on day 69 and sacrificed. The antibodies directed against CpnT$_{CTD}$ were purified from the antiserum of the animal PA4158: in a first step all the IgG contained in the antiserum were salted out using ammonium sulfate. The precipitated IgGs were solvated in Borate Buffer Saline buffer (BBS) and separated by affinity purification using recombinant $_{G818V}$CpnT$_{651-846}$ cross-linked to agarose beads. Extensive washing steps with BBS buffer removed unbound IgGs and the elution was performed using a step-wise pH gradient into neutralizing buffer. Antibodies from different pH fractions were pooled and concentrated to a final volume of 11 mL. 50% glycerol was added to enable long-term storage at -30ºC. *Mtb* ML1501 and ML1504 cultures were grown in 10 ml of 7H9/OADC/Tyloxapol media until OD_{600} reached 0.8-1. New cultures were re-inoculated into 150 ml of Sauton's media supplemented with Tyloxapol at an OD_{600} of 0.05, and grown until the OD_{600} reached .2. Cells were washed with sterile PBS to remove detergent, and re-inoculated into 150 ml of Sauton's media without detergent. After 4 days of growth, cells were centrifuged, and washed with PBS. The supernatant was filtered through a 0.22 µm filter and concentrated at least 200-fold using Amicon 3 kDa concentration tubes (Millipore). Cells were disrupted using Lysing Matrix B tubes (MP Biomedicals). Equal protein loads of the whole cell lysate (WC) and culture filtrate fractions (CF), as determined by the BCA protein assay (Pierce), were subjected to Western blotting using specific antibodies raised against polyclonal rabbit anti-CpnT$_{CTD}$ antibody and CFP10 antibody (Colorado State University), or monoclonal mouse anti-RNA polymerase (RNAP) β subunit (Neoclone), GroEL2 (Colorado State University), or AtpB (Abcam) antibodies. A horseradish peroxidase-coupled goat anti-mouse antibody (Sigma) and goat anti-rabbit antibody (Sigma) were used as secondary antibodies. Blots were developed using SuperSignal West Femto Western blotting substrate (Pierce).

Cell lines and cell culture. The Jurkat-derived cell line J644 stably expressing a doxycycline-controlled combined repressor/activator switch featuring the second generation Tet-transregulators rtTA2^S-M2 and tTS^D-PP and a J644-derived stable cell line encoding an activated form of caspase-3 (revCasp-3; (19)) have been described (20, 21).

HEK293T cells (from Dr. Sunnie Thompson, University of Alabama at Birmingham), C2C12 cells (ATCC CRL-1772), and RAW 264.7 cells (ATCC TIB-71) were propagated in Dulbecco's modified Eagle's medium (DMEM) supplemented with 10% fetal bovine serum (FBS), 2 mM Glutamax (Invitrogen), 50 U ml^{-1} penicillin, and 50 µg ml^{-1} streptomycin. THP1 cells (ATCC TIB-202) and Jurkat-derived cell lines were grown in RPMI-1640 medium supplemented with 10% FBS, penicillin, streptomycin and glutamine. All cells were grown in a 37°C humidified incubator at 5% CO_2.

Generation and imaging of a Jurkat-derived cell line stably expressing $CpnT_{CTD}$. J644 cells (Jr2^{S}M2PP; (20)) were transfected in 6-well dishes with 4 µg of AhdI-linearized pWHE655-$CpnT_{CTD}$ plasmid DNA using DMRIE-C (Invitrogen). J644-$CpnT_{CTD}$ cells were selected with 1200 µg/ml G418 (PAA Laboratories) for 14 days. Resistant cells were separated in 96-well plates (one cell per well) using a cell sorter (MoFlo, DakoCytomation) and cultured in selection medium with 2.5 µg/ml puromycin and 1200 µg/ml G418. After approximately 2 weeks, each individual clone was expanded into two wells of a 24-well plate, one with and one without doxycycline (1 µg/ml). Cell clones which quantitatively showed cell death in the presence of doxycycline, when microscopically analyzed, were further expanded. J644-derived cells expressing $cpnT_{CTD}$ were seeded at a density of 1 x 10^5 cells/ml in 24-well plates (0.5 ml). Cells were then either left uninduced or induced with 100 ng/ml doxycycline for 16 h. Cells were harvested by low-speed centrifugation and resuspended in PBS containing 1% FBS, and stained with 7-amino-actinomycin D (7AAD, eBioscience) according to the manufacturer's recommendation. Thereafter, the cells were allowed to settle to the bottom of the well and examined by fluorescence microscopy using an Axiovert 200 microscope (Carl Zeiss) equipped with a 100x/1.4 Plan-Apochromat and 40x/0.6 LD Plan-NEOFLUAR objectives (Carl Zeiss). Images were recorded using an AxioCam MRc camera (Zeiss) coupled to Axiovision v4.5 software (Carl Zeiss).

Transient transfection of HEK293T and C2C12 cells with a $cpnT_{CTD}$ expression vector. Transfection experiments were done for C2C12 at 80–90% confluence. The plasmids pML2093 and pML2138 were used for transient transfection of wt $cpnT_{CTD}$ and the $cpnT_{CTD}$ encoding the G818V mutant, respectively. Cells were trypsinized, re-plated onto collagen-I (6.7 µg cm^{-2}) coated plates, and immediately transfected with Lipofectamine 2000 (Invitrogen) and 2 µg of corresponding plasmid per the manufacturer's instructions. HEK293T cells were transfected while adherent. 24 hours after transfection, the cell morphology was analyzed using a Nikon Eclipse Ti microscope (magnification x 20). To analyze protein expression, cells were harvested in RIPA buffer (50 mm Tris-HCl pH 7.4, 150 mm NaCl, 1 mm EDTA, 1% NP-40, 0.5% sodium deoxycholate, and 0.1% SDS) and homogenized with repeated pipette tip flushing. Lysates were centrifuged at 5,000 x *g* for 5 min and equal protein loads of the soluble fraction, as determined by the BCA protein assay (Pierce), were subjected to Western blotting using anti-HA and anti-actin antibodies (Cell Signaling Technology, Inc., Danvers, MA, USA).

Measurement of cell death by flow cytometry in J644-derived cell lines. The characterization of cell death was done by flow cytometry employing a 4-color-staining procedure established and standardized in the lab (22). This procedure allows the characterization of six different phases of cell death by detecting various biologically-relevant changes in the cells: the exposure of phosphatidyl serine (PS), the ion permeability of the plasma membrane, the mitochondrial membrane potential, the transmembrane transporter function, and DNA-content. For staining, we used a fluorescent PS ligand (Annexin-A5-FITC; responsif, Erlangen, Germany), a membrane impermeable fluorescent ion (propidium iodide; Sigma), a membrane-potential-sensitive 1,1′,3,3,3′,3′-hexamethylindodicarbo-cyanine iodide dye ($DiIC_1(5)$; Invitrogen), and the fluorochrome 2,5'-Bi-1H-benzimidazole, 2'-(4-ethoxyphenyl)-5-(4-methyl-1-piperazinyl) (Hoechst 33342; Molecular Probes, Leiden, The Netherlands) to detect functional export of this compound and DNA-content. The cells were classified into viable (V), early apoptosis/apoptosis/late apoptosis (EA/A/LA), secondary necrosis/late secondary necrosis (SN/LSN) and primary necrosis (PN) according to their staining properties and their location in the forward scatter (FSC; apparent size) / side scatter (SSC; granularity) plots. The Jurkat-derived cells were seeded in a 12-well-plate at a density of 1×10^5 cells/ml 24 h before adding doxycycline to a final concentration of 1 µg/ml to the medium to induce cell death. They were then incubated at 37°C, 5% CO_2 and 95% humidity. Before each measurement, the cell suspension was thoroughly mixed by repeated up- and down-pipetting. 100 µl of this suspension were transferred to a 5 ml round bottom tube (Falcon) which already contained 400 µl freshly prepared 4-color-staining solution [1 µg/ml Annexin-A5-FITC, 20 µg/ml PI, 10 nM $DiIC_1(5)$, 1 µg/ml Hoechst 33342) in Ringer`s solution (Delta Select, Pfullingen, Germany)] and subsequently analysed by flow cytometry with a Gallios cytofluorometer (Beckman-Coulter, Krefeld, Germany). Excitation for FITC and PI was at 488 nm; FITC fluorescence was recorded with the FL1 sensor (525/38 nm BP), PI fluorescence with the FL3 sensor (620/30 nm BP). The $DiIC_1(5)$ fluorescence was excited at 638 nm and recorded with the FL6 sensor (675/20 nm BP). The Hoechst 33342 fluorescence was excited at 405 nm and recorded with the FL9 sensor (430/40 nm BP). Electronic compensation was

used to eliminate bleed-through fluorescence. Data analysis was performed with Kaluza software, version 1.2 (Beckman-Coulter).

Inhibition of cell death. Six hours prior to measurement, J644-derived cell lines were seeded at a density of 1-2 x 10^5 cells/ml in 12-well plates (2 ml). One hour prior to measurement, inhibitors were added in the concentrations shown in the Table S4. Doxycycline was applied at t=0. Measurements were carried out as described in the flow cytometry section.

Measurement of DNA content in nuclei of J644-derived cell lines. DNA fragmentation in nuclei was determined using a published protocol (23). The Jurkat cell lines J644-revCasp-3 and J644-CpnT$_{CTD}$ were seeded in six-well plates at a concentration of 1-2x10^5 cells per milliliter (3ml total volume). Cell death was induced by addition of 1µg/ml doxycycline. At each assay point, the cell suspension was thoroughly resuspended by pipetting. 100µl of this solution were then transferred to round bottom tubes (5ml), which contained 400µl of PI-Triton solution (0.1% trisodium citrate, 0.1% Triton X-100, 1µg/ml PI (all Sigma-Aldrich)). The mix was incubated for 12-24h at 4°C to ensure total disassembly of the plasma membrane. The nuclei were analyzed with an EPICS XL flow cytometer (Beckman-Coulter) and the data was processed with the software Kaluza 1.2 (Beckman-Coulter). The gating strategy gated for intact nuclei and excluded doublets, i. e. nuclei or cells sticking together which would skew the DNA content in the G0, S or G2/M phases.

Role of Rv3903c for cytotoxicity and survival of *Mtb* in macrophages. THP-1 macrophages were seeded on 24-well plates (0.5 x 10^6 cells/well) and differentiated overnight with 50 ng/mL 12-phorbol 13-myristate acetate (PMA). Macrophages were washed and replenished with culture media without antibiotics 2 h prior to infection with *Mtb* strains. *Mtb* strains growing in mid-log phase were normalized by optical density (OD_{600} 1.0 = 3 x 10^8 bacteria), washed and opsonized in infection media containing 20% normal human serum (Millipore) for 30 min at 37°C. Macrophages were then infected with live or heat-killed ML1528 (wild-type), ML2000 (*Mtb* Δ*cpnT*), ML2001 (*Mtb* Δ*cpnT::p$_{imyc}$-esxF-esxE-cpnT-rv3902c),* or ML2002 *(Mtb* Δ*cpnT::p$_{imyc}$-esxF-esxE-cpnT$_{NTD}$-rv3902c)* at a multiplicity of infection (MOI) of 20 or 10 to assess cytotoxicity or intracellular survival, respectively. Macrophage monolayers were then washed 3 times with PBS 3 h post-infection and replenished with culture media. Thereafter, macrophage viability was assessed 48 h post infection by staining with Live/Dead Fixable Green Cell Stain (Invitrogen) according to manufacturer's recommendation. Cells were then analyzed by flow-cytometry (Guava easyCyte) to assess the percentage of dead cells as indicated by positive green signal (FL1). To assess intracellular survival of *Mtb* strains, infected macrophages were incubated for the indicated time points and bacteria were harvested after macrophage lysis in 0.025% SDS. Both attached (viable) and detached (non-viable) macrophages were collected to ensure all *Mtb* cells were accounted for. Serial dilutions of recovered bacteria were then plated on solid 7H10 media supplemented with 10% OADC and kanamycin. CFU counts were performed after 3 weeks of incubation at 37°C.

Mouse experiments. Eight-week-old female C57BL/6 mice (Jackson Laboratories) were infected by aerosol using an Inhalation Exposure System (Glas-Col) and early-log-phase cultures of the *Mtb* strains ML812, ML1504 and ML1518 as single-cell suspensions in PBS to deliver approximately 100 bacilli per mouse. Serial dilutions of organ homogenates from four mice per data point were plated onto 7H10 agar plates to quantify CFUs. Experiments involving mice were reviewed and approved by the Institutional Animal Care and Use Committee of Weill Cornell Medical College.

Statistical analysis. Data are presented as mean ± standard deviation; *p* values were calculated using the Student's *t* test and a *P* value of <0.05 was considered to be significant.

SUPPLEMENTARY FIGURES

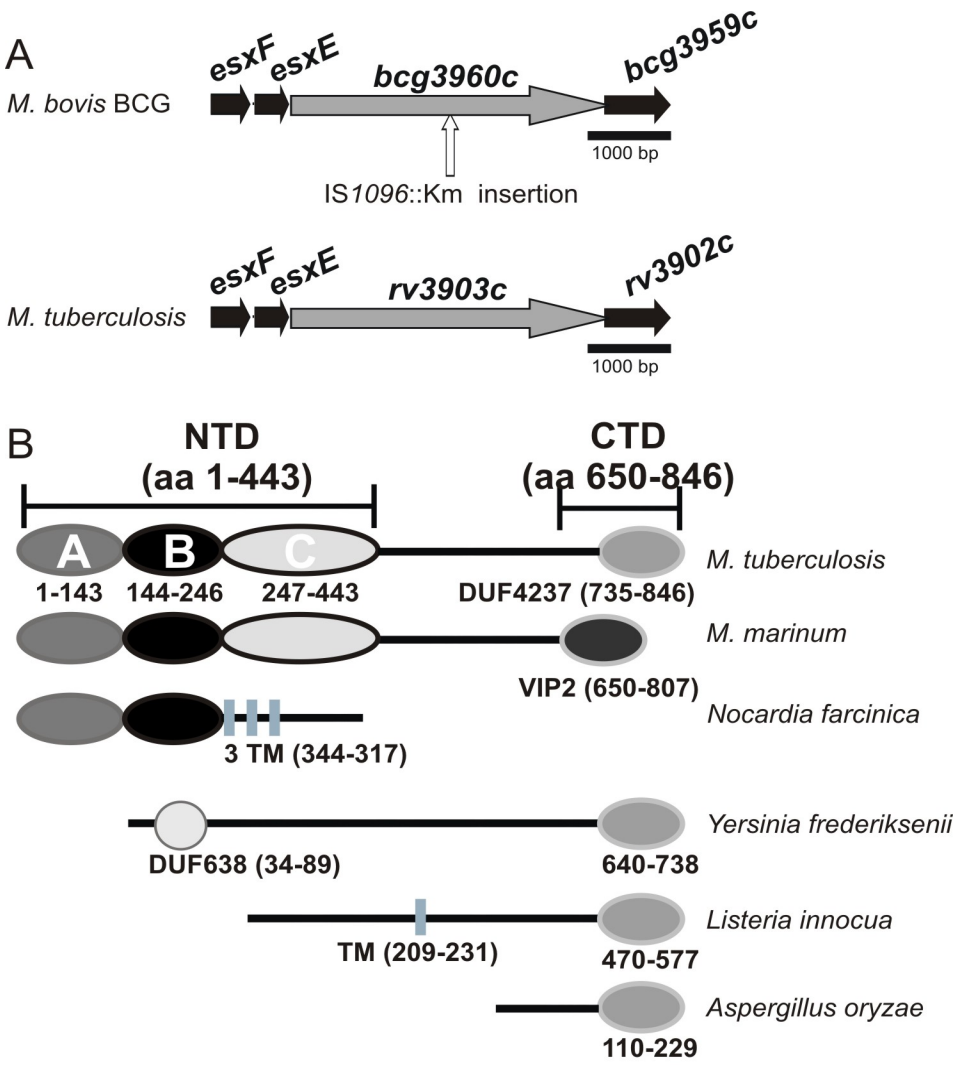

Figure S1. Bioinformatic analysis of Rv3903c (CpnT) of *M. tuberculosis*. A. Genomic regions of *bcg3960c/rv3903c* in *M. bovis* BCG and *Mtb*, respectively. The vertical arrow depicts the insertion of the transposon in the *M. bovis* BCG mutant ML1012. Horizontal arrows represent open reading frames. Rv3902c, hypothetical protein; EsxE, EsxF, putative ESAT-6 like proteins. **B**. BLAST analysis in combination with secondary structure analysis prediction suggest that CpnT is a multidomain protein. Region A (aa 1-143) is an independent full-length protein in many Actinomycelates, but not in mycobacteria. Region B (aa 144-246) has similarity not only in mycobacteria, but also in Nocardia. Region C (aa 247-443) is predicted to have the highest amphiphilicity and beta sheet content (Fig. S6) and is present exclusively in mycobacteria. Regions A-C were named as a CpnT N-terminal domain throughout the text. The N-terminal domain (NTD, aa 1-443) is connected to the C-terminal domain (CTD, aa 650-846) by an Ala-Pro-rich linker region of low complexity (aa 449-649). The CTD of Rv3903c contains the uncharacterized DUF4237 family motif. DUF4237 is found in bacteria and eukaryotes. VIP2: ADP-ribosylating toxin family; TM: transmembrane helix.

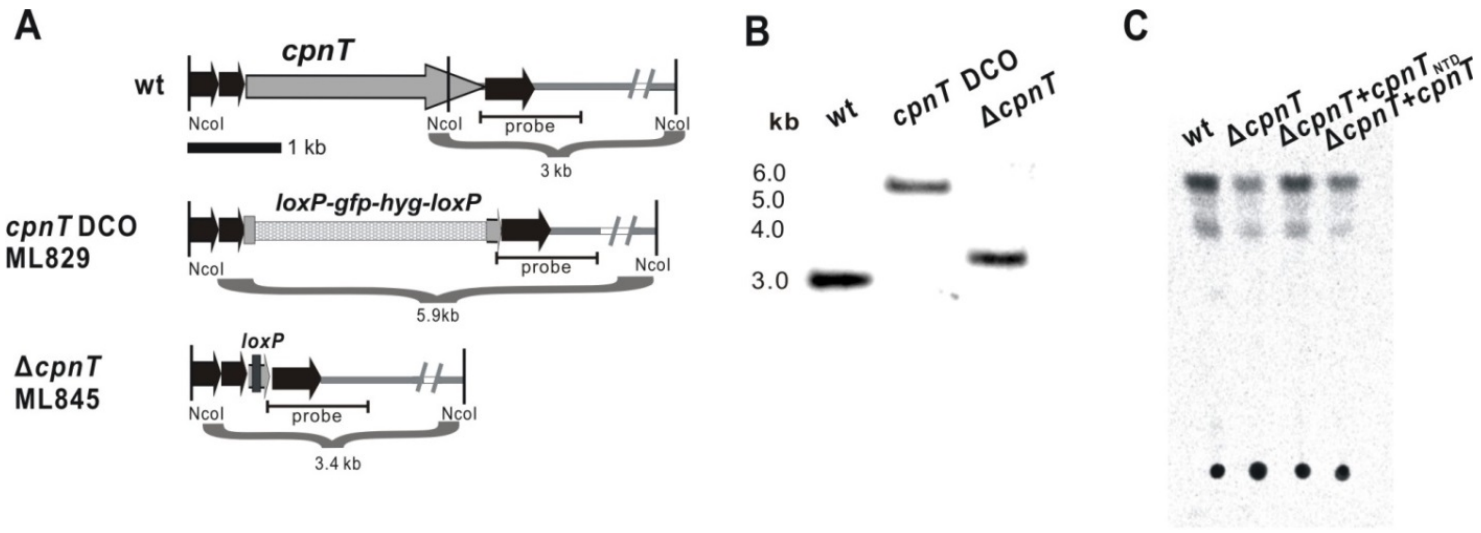

Figure S2. Construction of the *cpnT* deletion mutant in *M. tuberculosis* H37Rv.

A. Schematic representation of the chromosomal region of *cpnT* in wt *Mtb*. Genes are drawn to scale. The probe used for Southern Blot analysis is indicated. A two-step selection process was used to obtain the marked double crossover in strain ML829 (*cpnT* DCO). *Mtb* H37Rv was initially transformed with a temperature-sensitive replicative knock-out vector. Positive clones were screened for the presence of *hyg*, *gfp*, and *xylE* genes. Counterselection against *sacB* yielded the double crossover clone ML829 that was selected based on the presence of *gfp* and *hyg*, and absence of *xylE* and *sacB*. The *loxP* flanked *gfp-hyg* cassette was removed by Cre recombinase to create the unmarked mutant ML845 (Δ*cpnT*).

B. Genomic DNA of *Mtb* was digested with NcoI and analyzed by Southern blotting using the probe indicated in Fig. S2A. kb, molecular mass makers in kilobases.

C. Phthiocerol dimycocerosate (PDIM) analysis of wt *Mtb* (lane 1), Δ*cpnT* (lane 2), and Δ*cpnT* complemented with $CpnT_{NTD}$ (lane 3), or CpnT (lane 4). *Mtb* lipids were labeled with [^{14}C]-propionic acid.

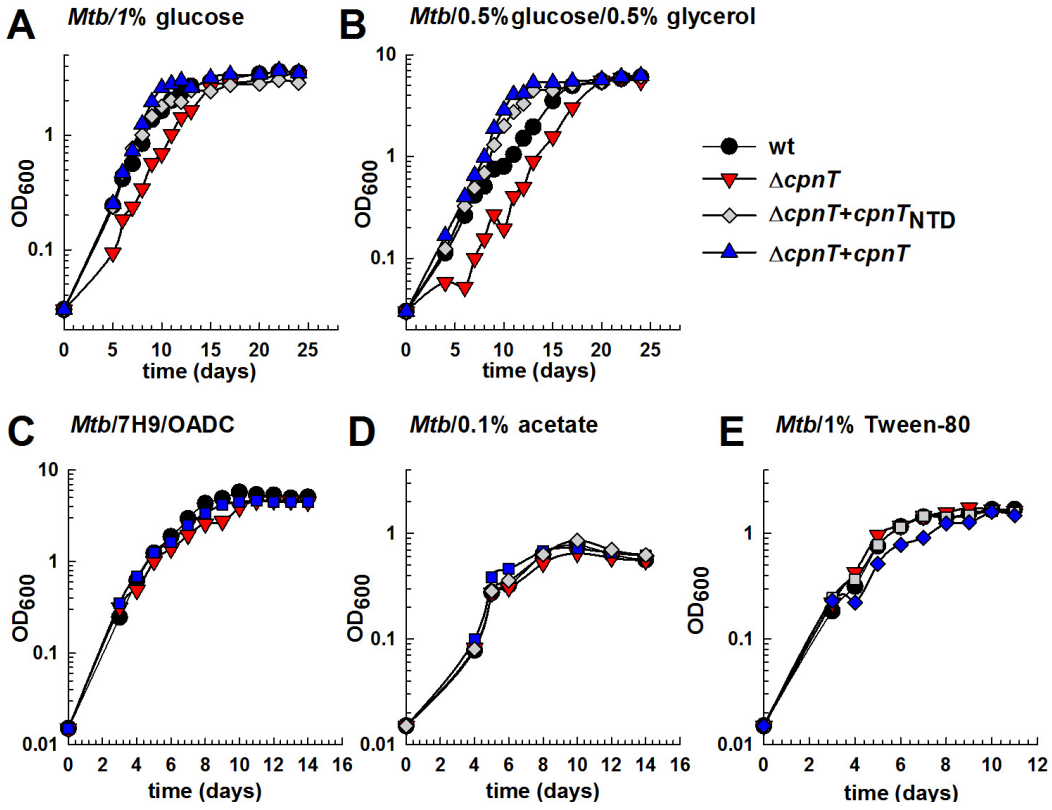

Figure S3. CpnT is required for efficient utilization of glycerol and glucose by *M. tuberculosis*. Growth of wt *Mtb* (●), Δ*cpnT* (▼), and Δ*cpnT* complemented with $cpnT_{NTD}$ (◆), or *cpnT* (▲) in 7H9 with various carbon sources. **A.** 1% glucose, **B.** 0.5% glucose and 0.5% glycerol, **C.** OADC, **D.** 0.1% acetate, **E.** 1% Tween-80. Experiments were carried out at least three independent times, a representative growth curve is shown for each case.

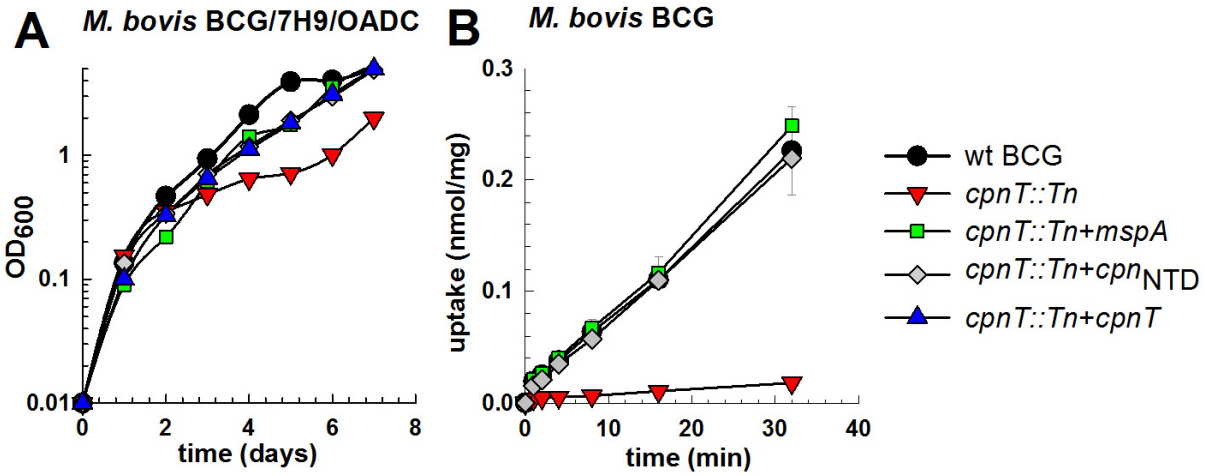

Figure S4. The N-terminal domain of CpnT is sufficient for efficient growth *in vitro* and uptake of glycerol by *M. bovis* BCG. A. Growth of wt *M. bovis* BCG (●), *cpnT*::*Tn* (▼), *cpnT*::*Tn* complemented with *mspA* (■), $cpnT_{NTD}$ (◆), or *cpnT* (▲) in 7H9/OADC. Experiments were carried at least three independent time, representative growth curves are shown. **B.** [^{14}C] Glycerol uptake experiments for wt *M. bovis* BCG (●), *cpnT*::*Tn* (▼), *cpnT*::*Tn* complemented with *mspA* (■), and $cpnT_{NTD}$ (◆). The uptake rate is expressed as nmol of glycerol per milligram of cells. The uptake experiment was done in triplicate and is shown with standard deviations. The *p*-value determined by a Student t-test was less than 0.05 for wild-type vs. the *cpnT*::*Tn* mutant for all time points.

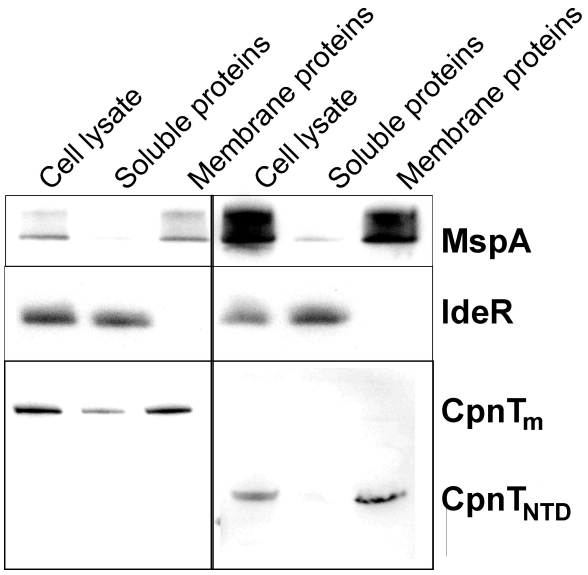

Figure S5. CpnT is a membrane protein in *M. smegmatis*. *M. smegmatis* mc^{2}155 strain was transformed with plasmid expressing the NTD of CpnT (pML2040) or full length CpnT with a non-toxic G818V mutation ($CpnT_m$; pML2172). The cytoplasmic protein IdeR and the outer membrane protein MspA were used as controls for subcellular fractionation. CpnT was expressed with a C-terminal fusion of the Human influenza hemagglutinin (HA) tag which was detected using an HA-specific antibody.

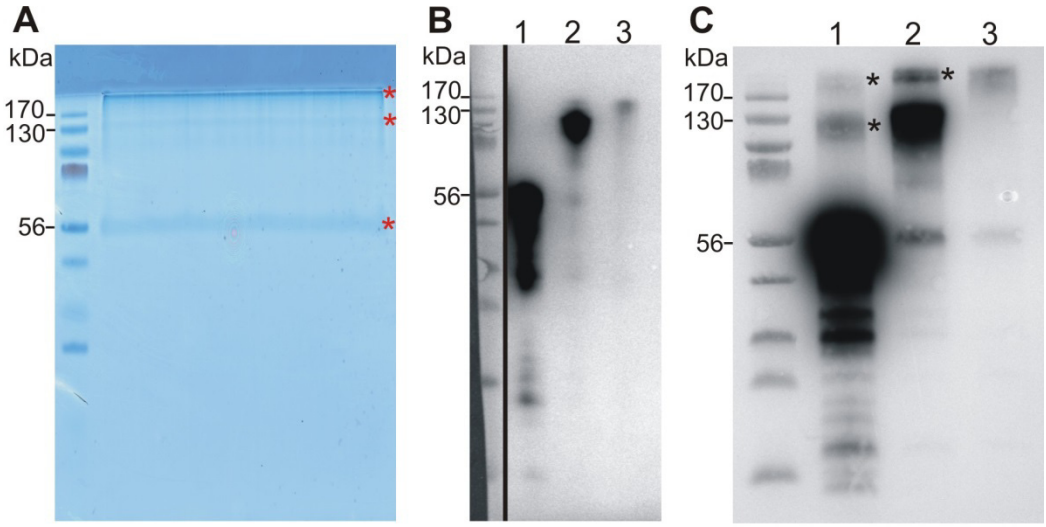

Figure S6. Purification of monomers and oligomers of $CpnT_{NTD}$. A. Gel extraction of $CpnT_{NTD}$. After nickel affinity and anion exchange chromatography, the protein sample was concentrated and separated on a 10% SDS-polyacrylamide gel. To preserve disulfide bridges in $CpnT_{NTD}$, the protein was mixed with non-reducing loading buffer and immediately loaded on a gel without boiling. The gel was stained with Simple Blue Safe Stain (Invitrogen) which does not require fixation. Three bands corresponding to different oligomeric forms of $CpnT_{NTD}$ (~56 kDa, ~130 kDa, ~200 kDa) were cut from the gel (red asterisks). **B, C.** Western blot analysis of different oligomeric forms of $CpnT_{NTD}$ after gel extraction. The excised proteins were mixed with a non-reducing loading buffer and loaded onto a 10% SDS-polyacrylamide gel directly after elution **(B)**, or after refolding at room temperature for one week in the presence of 0.5% octyl-POE **(C)**. Proteins were transferred to a PVDF membrane and detected with anti-HA-HRP-conjugated antibodies. Gels were loaded with samples containing the excised bands of ~56 kDa (lanes 1), ~130 kDa (lanes 2) and ~200 kDa (lanes 3). Larger, oligomeric forms of $CpnT_{NTD}$ in the samples of the monomer (~56 kDa) and the ~130 kDa form (C, lanes 1 and 2) that appeared after incubation for one week with detergents are marked by asterisks.

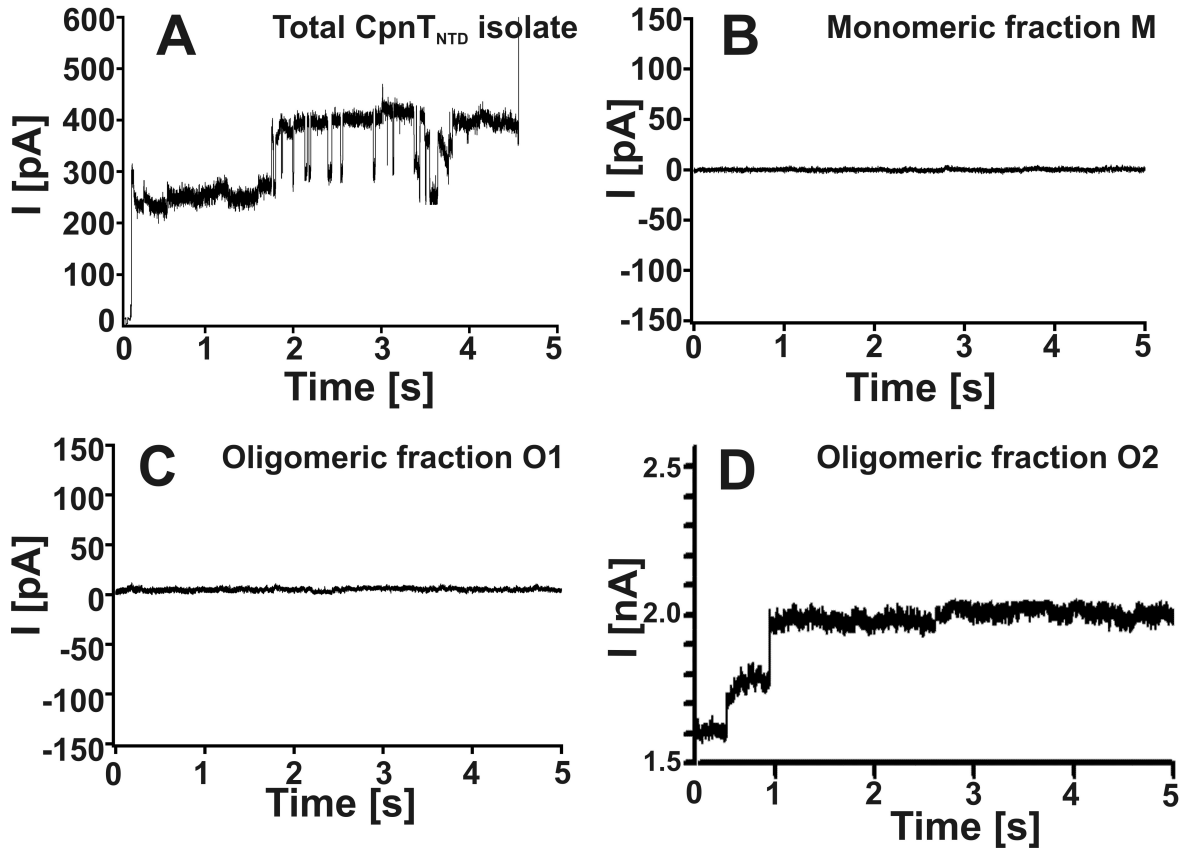

Figure S7. Channel activity of different forms of the N-terminal domain of CpnT.
Current traces of purified CpnT$_{NTD}$ reconstituted into giant unilamellar vesicles (GUV) **(A)**, of the CpnT$_{NTD}$ monomer (~56 kDa) **(B)**, of the CpnT$_{NTD}$ O1 oligomer (~130 kDa) **(C)** and of the CpnT$_{NTD}$ O2 oligomer (~200 kDa) **(D)**. Bands corresponding to different forms were excised and eluted from the gel. The protein samples were then added to the lipid bilayer. The channel insertions in D had currents/conductances of 106 pA/1 nS and 178 pA/1.8 nS. All current traces were recorded at +100 mV. The protein concentration in all experiments was approximately 0.3 µg/ml.

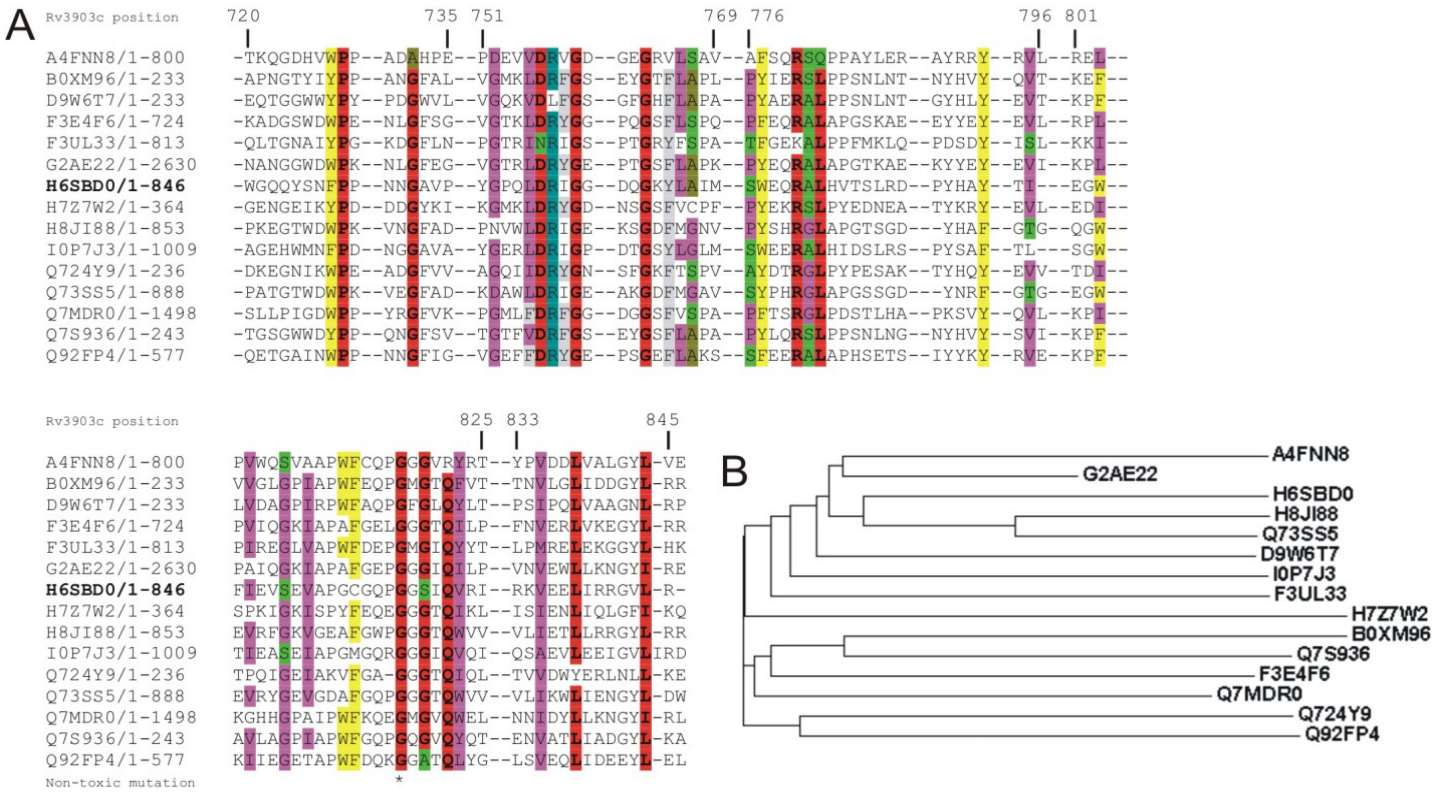

Figure S8. Alignment of proteins with similarity to the CpnT toxin domain of *M. tuberculosis*. Cell wall surface anchor family protein A4FNN8 from *Saccharopolyspora erythraea*; Hemagglutinin repeat family protein G2AE22 from *Escherichia coli* STEC; uncharacterized proteins H6SBD0 from *Mycobacterium tuberculosis*, H8JI88 from *Mycobacterium intracellulare*, Q73SS5 from *Mycobacterium paratuberculosis*, D9W6T7 from *Streptomyces himastatinicus*, I0P7J3 from *Mycobacterium abscessus*, F3UL33 from *Streptococcus sanguinis*, H7Z7W2 from *Campylobacter jejuni*, B0XM96 from *Neosartorya fumigata*, Q7S936 from *Neurospora crassa*; hemagglutinin repeat-containing protein F3E4F6 from *Pseudomonas syringae*; Rhs family protein Q7MDR0 from *Vibrio vulnificus*; putative uncharacterized proteins Q724Y9 from *Listeria monocytogenes* strain F2365 and Q92FP4 from *Listeria innocua* strain CLIP 11262.

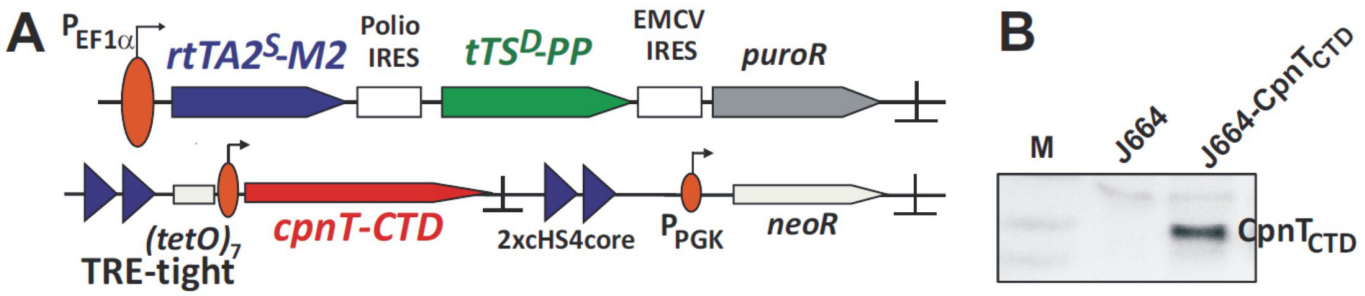

Figure S9. Tetracycline-controlled *cpnT$_{CTD}$* expression in Jurkat T cells.
A. Schematic overview of the constructs used in the regulatory system. The regulator construct is displayed on top. A human EF-1α promoter (red oval with broken arrow) constitutively transcribes a tricistronic mRNA. The mRNA contains the reverse transactivator rtTA2^{S}-M2 (blue), the transsilencer tTS^{D}-PP (green) and a selection marker (puromycin resistance; grey). Translation of the latter two genes is mediated by internal ribosome entry sites (IRES; open boxes) from Polio-virus and Encephalomyocarditis-virus (EMCV). The bottom vector contains the response unit. It features the *cpnT*$_{CTD}$ target gene (red) driven by the Tet-responsive promoter TREtight (open box, red oval with broken arrow) and flanked by 2 repeats each of a 250 bp sequence from the chicken HS4 insulator (blue triangles). A murine phosphoglycerate kinase 1 promoter (PGK; red oval with broken arrow) drives expression of a gene mediating G418-resistance (neoR). PolyA sites in all vectors are marked by a "⊥".
B. Tetracycline-controlled *cpnT$_{CTD}$* expression in the Jurkat J644-*cpnT*$_{CTD}$ cell line. Cells were lysed 16 h after induction with doxycycline. CpnT$_{CTD}$ was detected in the cell lysates in an immuno-blot using the purified specific polyclonal antiserum against the C-terminal domain of CpnT. The parent cell line Jurkat J644 served a control. Both cell lines were induced with 100 ng/mL doxycycline.

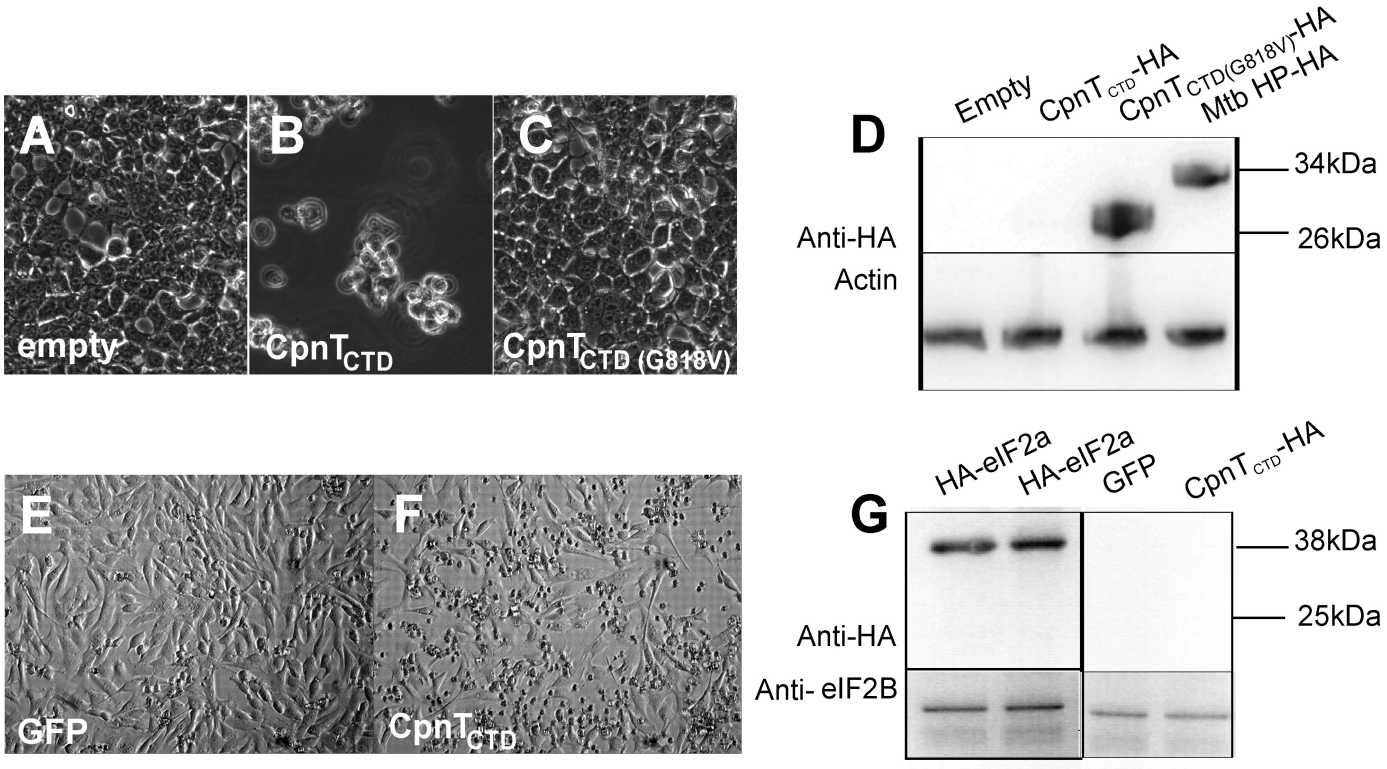

Figure S10. Survival of human embryonic kidney 293T cells (**A-C**) and mouse myoblast C2C12 cells (**E** and **F**) 24 hours after transient transfection with empty vector (**A**), and vectors expressing wt *cpnT*$_{CTD}$ (**B** and **F**), the non-toxic mutant *cpnT*$_{CTD(G818V)}$ (**C**), or a *gfp*-containing control vector (**E**). The experiment was done two independent times and representative images are shown. Transfection efficiency of HEK293T and C2C12 cells were 95% and 70% respectively, which was determined using a *gfp*- expression vector control done in parallel with transfections using a *cpnT*$_{CTD}$ expression vector. (**D, G**). Immunoblot experiments were performed to determine the CpnT$_{CTD}$ protein level in cells 24h after transfection. A C-terminal HA-tag was introduced for CpnT detection by an HA-specific antibody. Actin and EIF2B proteins were used as loading controls. We used an unrelated *Mtb* hypothetical protein with unknown function (labeled here as *Mtb* HP-HA) as a control for protein expression and toxicity. No cell death was detected in cells transfected with an empty vector and an *Mtb* HP-HA construct. In these experiments the *cpnT*$_{CTD}$ gene is transcribed from the constitutive CMV promoter. This leads to early cell death and detachment of cells from the monolayer. Since only live cells were used for the cell lysates, they were probably not transfected and/or did not express *cpnT*. Thus, CpnT is not detected in these cells.

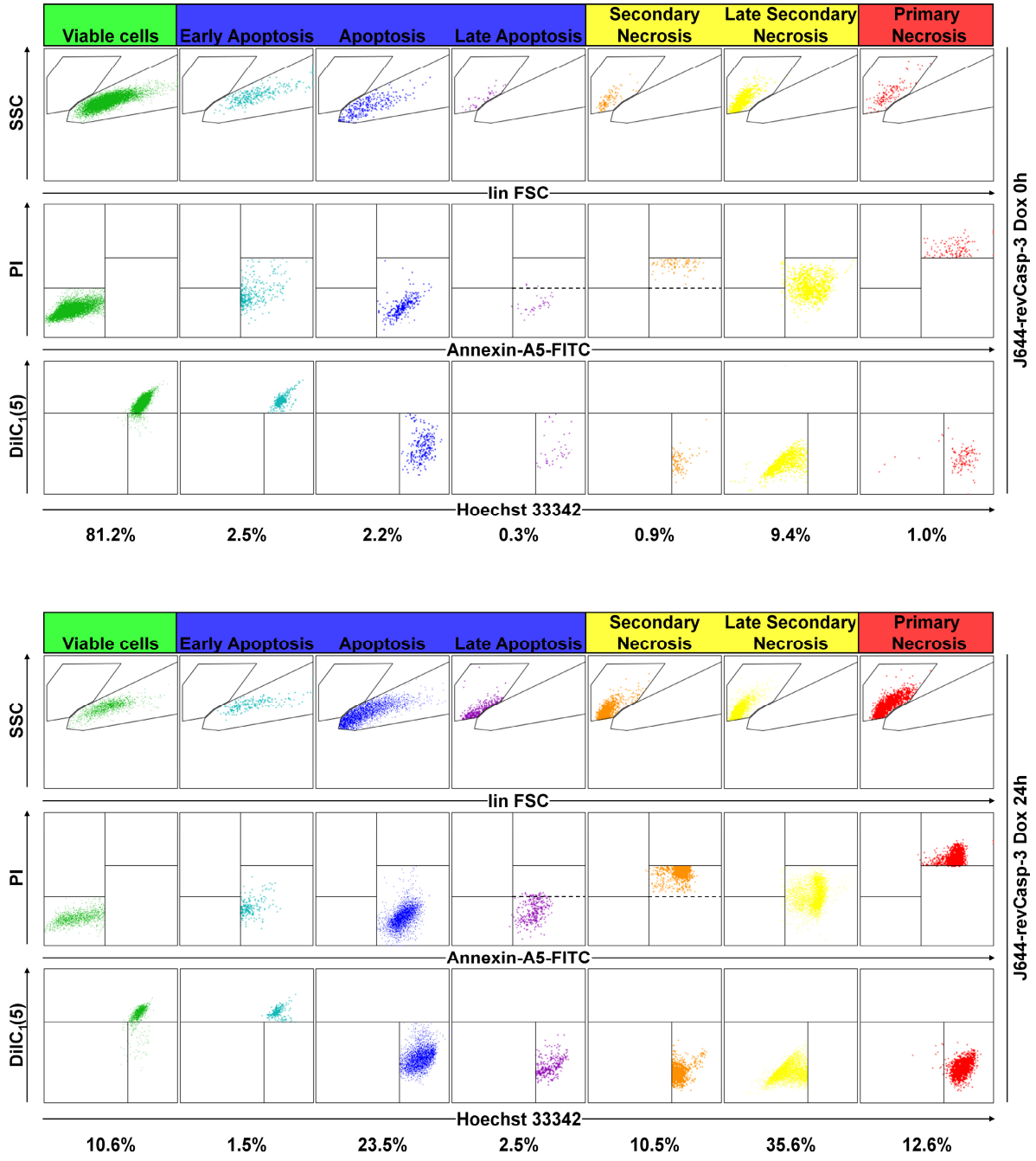

Figure S11. Flow cytometry of a Jurkat T-cell line expressing a gene encoding activated caspase-3. The Jurkat J644-derived cell line expressing a gene encoding the activated caspase-3 (revCasp-3) was cultured for 24 h in the presence of 1 µg/ml doxycycline, harvested, stained according to the 4-color-protocol and analyzed by flow cytometry (Gallios, Beckman-Coulter, Krefeld, Germany). Shown are FSC vs. SSC, Annexin-A5 vs. PI and $DiIC_1(5)$ vs. Hoechst 33342 dot plots. The signals obtained are used to (i) separate the cells according to their apparent size (FSC) and surface granularity (SSC) for distinguishing between cells with a phenotype typical for viable or dead cells (top plots), (ii) determine the surface exposure of phosphatidylserine (Annexin-A5-FITC) and the plasma-membrane integrity (PI) to distinguish between apoptotic, primary and secondary necrotic cells (middle plots), and (iii) measure the mitochondrial membrane potential [$DiIC_1(5)$] and the degree of nuclear DNA fragmentation (Hoechst 33342) to distinguish between primary and late secondary necrotic cells (bottom plots). PI fluorescence intensity is additionally grouped into “intermediate” and “low” (highlighted by the dotted line) to better distinguish between late apoptotic cells and secondary necrotic cells, which otherwise have identical properties in the staining protocol. The gates used to identify the various cell death phenotypes are indicated in the dot plots and the percentages of each population are given below each set of plots.

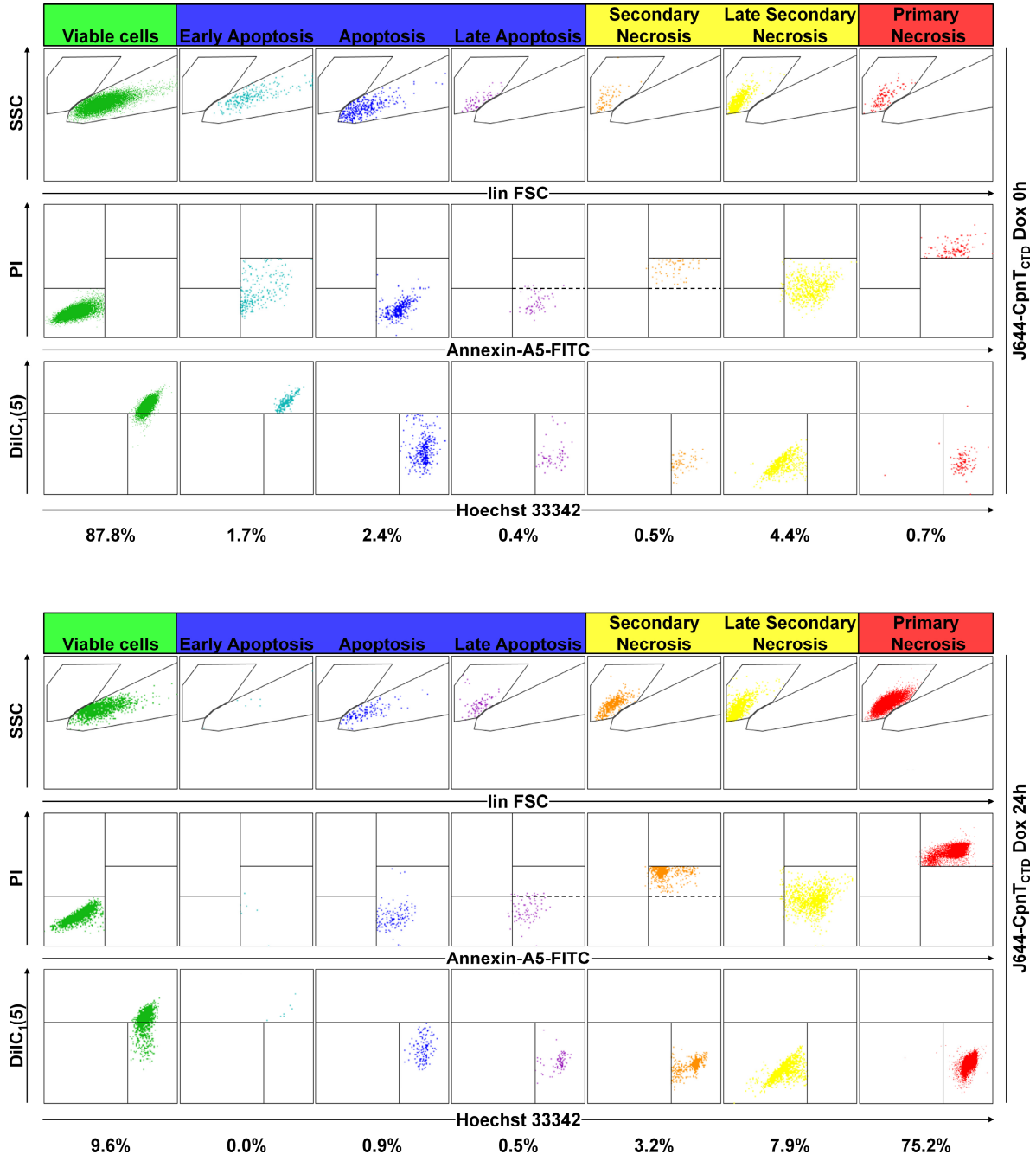

Figure S12. Flow cytometry of a Jurkat T-cell line expressing *cpnT*$_{CTD}$. The Jurkat J644-derived cell line expressing *cpnT*$_{CTD}$ was cultured for 24 h in the presence of 1 µg/ml doxycycline, harvested, stained according to the 4-color-protocol and analyzed by flow cytometry (Gallios, Beckman-Coulter, Krefeld, Germany). Shown are FSC vs. SSC, Annexin-A5 vs. PI and DiIC$_1$(5) vs. Hoechst 33342 dot plots. The signals obtained are used to (i) separate the cells according to their apparent size (FSC) and granularity (SSC) for distinguishing between cells with a morphology typical for viable or for dead cells (top plots), (ii) determine the surface exposure of phosphatidylserine (Annexin-A5-FITC) and the plasma-membrane integrity (PI) to distinguish between apoptotic, primary and secondary necrotic cells (middle plots), and (iii) measure the mitochondrial membrane potential [DiIC$_1$(5)] and the degree of nuclear DNA fragmentation (Hoechst 33342) to distinguish between primary and late secondary necrotic cells (bottom plots). PI fluorescence intensity is additionally grouped into “intermediate” and “low” (highlighted by the dotted line) to better distinguish between late apoptotic cells and secondary necrotic cells, which otherwise have identical properties in the staining protocol. The gates used to identify the various cell death phenotypes are indicated in the dot plots and the percentages of each population are given below each set of plots.

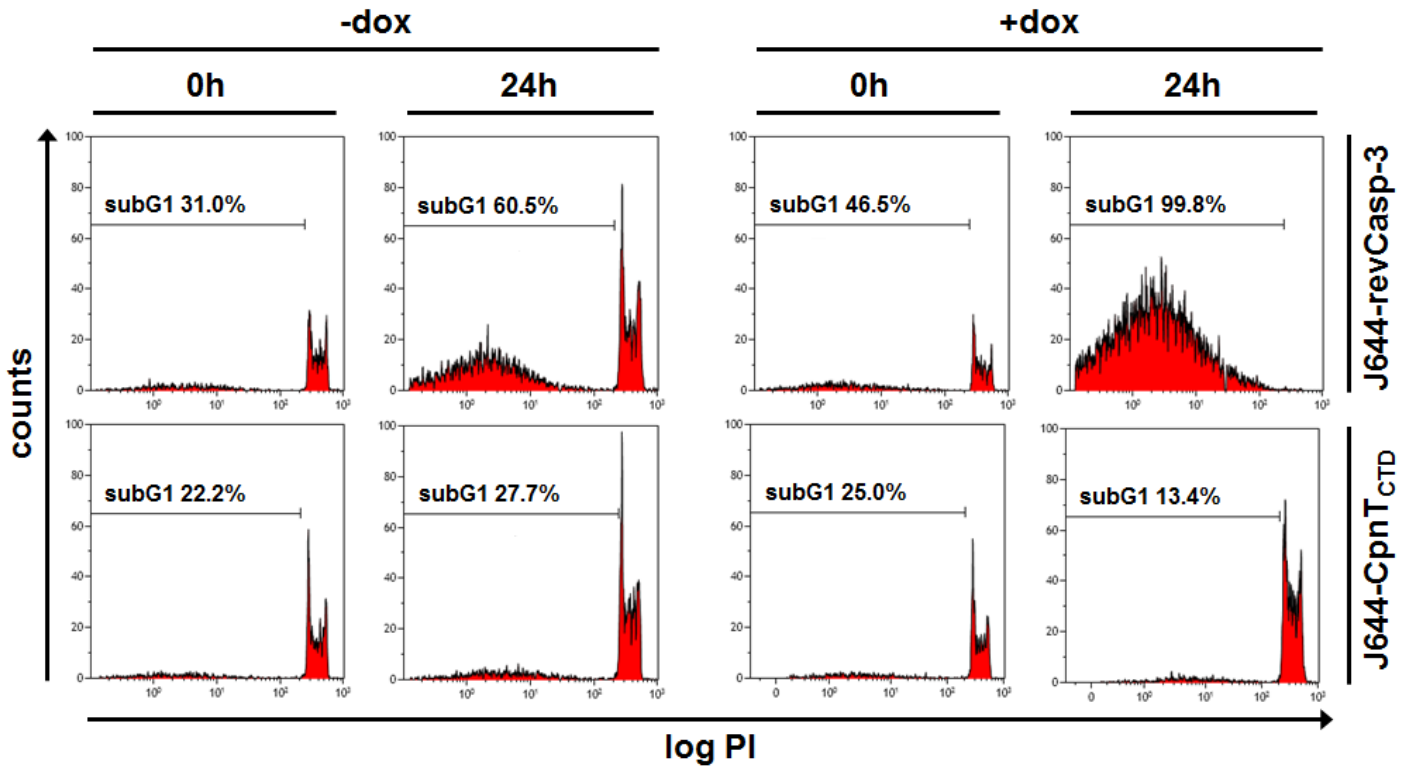

Figure S13. Cell death induced by Cpn$_{CTD}$ does not lead to nuclear DNA fragmentation.
The Jurkat cell lines J644-revCasp-3 and J644-CpnT$_{CTD}$ were grown in six-well plates with a concentration of 1-2x10^5 cells per milliliter (3 ml total volume). Cell death was induced by addition of 1 µg/ml doxycycline. At 0 and 24h after induction of transgene expression, the cell suspension was stained for 24 h at 4°C with PI-Triton solution (23), analyzed by flow cytometry (EPICS XL; Beckman-Coulter) and the data processed with the software Kaluza 1.2 (Beckman-Coulter). The gating strategy gated for intact nuclei, excluding doublets. The percentage of nuclei with fragmented DNA in the subG1 fraction is given above the respective cell population in each histogram.

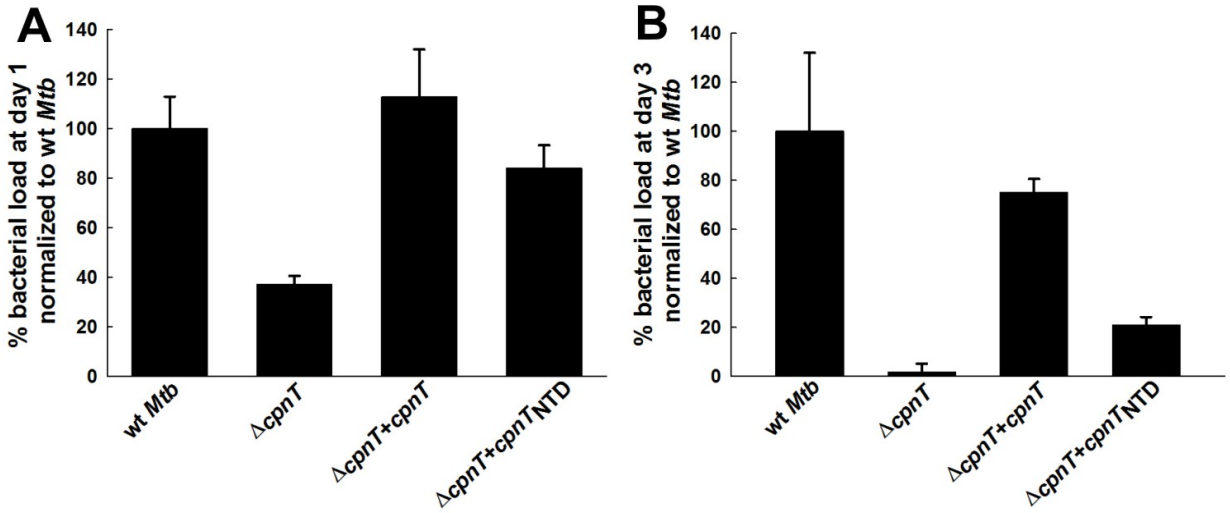

Figure S14. Role of CpnT in replication of *M. tuberculosis* in macrophages. The number of live, intracellular *Mtb* cells from macrophages at days 1 **(A)** and 3 **(B)** after infection were determined by plating on 7H10 Middlebrook agar plates as shown in Fig. 5B. The bacterial load was normalized to that of wt *Mtb*. 100% corresponds to approximately 3 x 10^6 and 4 x 10^7 bacteria on days 1 and 3, respectively.

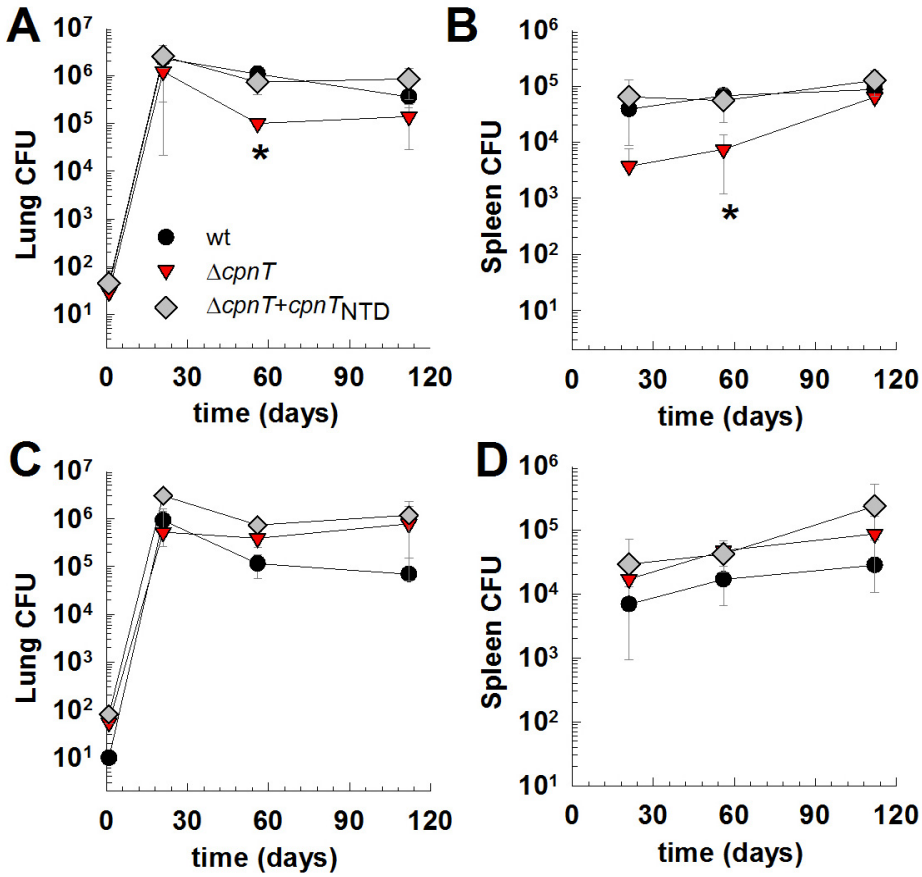

Figure S15. Infection of C57BL/6 mice with the *M. tuberculosis cpnT* deletion mutant. Bacterial loads in lungs (**A, C**) and spleens (**B, D**) from mice infected by aerosol with wt H37Rv (●), Δ*cpnT* (▼), and Δ*cpnT* complemented with the $cpnT_{NTD}$ expression vector pML2046 (⧫). Two independent experiments are shown in A, B and C, D. Data points represent means of four mice per group and error bars indicate the standard deviation from the mean. Survival of the wt vs. mutant, or complemented strains was analyzed using Student's t-test. * $p < 0.05$ was deemed significant.

SUPPLEMENTARY TABLES

Plasmid	Relevant genotype and properties	Source or reference
pCV125	ColE1 origin*, int,* L5 *attP, aph*, *lacZ*	(24)
pET21a(+)	T7 promoter, transcription start and terminator, His-tag, *lacI*, *bla*, pBR322 ORI, 5443 bp	Novagen, WI
pMN013	ColE1 origin, *hyg*, oriM, p_{imyc}-*mspA,* 6000 bp	(4)
pMN016	ColE1 origin, *hyg*, oriM, p_{smyc}-*mspA,* 6164 bp	(25)
pML113	FRT-*hyg*-FRT, *bla*, L5 *attP*, ColE1 origin, 4365 bp	(3)
pML515	pUC origin, pAL5000ts, *sacR*, *sacB, xylE,* up_*mctB*_hom*, loxP*-p_{imyc}-*mycgfp2*+-*hyg-loxP*, down_*mctB*_hom, 11859 bp	(26)
pMS2	ColE1 origin; PAL5000 origin; *hyg*; 5229 bp	(6)
pNIT-1::gfp	ColE1 origin, *aph*, oriM, p_{nit1}-*efgp*, p_{nit2}-*nitR*, 6912 bp	(5)
pMAL-c5X	pMB1 origin, *rop*, *bla*, *lacI*^{q}, p_{tac}-*malE*-POLYN-XA-MCS, 5677 bp	New England Biolabs, MA
pML1113	pUC origin, pAL5000ts, *sacR*, *sacB, xylE,* up_*cpnT*_hom*, loxP*-p_{imyc}-*mycgfp2*+-*hyg-loxP*, down_*cpnT*_hom, 11981 bp	This work
pML1828	ColE1 origin, pAL5000 origin, *hyg*, p_{smyc}-*mbtG-HA*, 6853 bp	(10)
pML1925	pMB1 origin, *rop*, *bla*, *lacI*^{q}, p_{tac}-HIS-*malE*-POLYN-XA-MCS, 5695 bp	This work
pML1947	pMB1 origin, *rop*, *bla*, *lacI*^{q}, p_{tac}-HIS-*malE*-POLYN-TEV-MCS, 5698 bp	This work
pML1950	pMB1 origin, *rop*, *bla*, *lacI*^{q}, p_{tac}-HIS-*malE*-POLYN-TEV-$_{G818V}$*cpnT*$_{651-846}$, 6233 bp	This work
pML2008	pBR322 origin, L5 *attP*, FRT-*hyg-int*-FRT, 5749 bp	This work
pML2009	pBR322 origin, L5 *attP*, FRT-*hyg-int*-p_{imyc}-*mspA*-FRT, 6676 bp	This work
pML2010	pBR322 origin, L5 *attP*, FRT-*hyg-int*-p_{imyc}-*rv3903c*-FRT, 8557 bp	This work
pML2023	pBR322 origin, L5 *attP*, FRT-*hyg-int*- p_{imyc}-*cpnT*-HA-His-FRT, 8613 bp	This work
pML2024	ColE1 origin, *aph*, oriM, p_{nit1}-*cpnT*-HA-His, p_{nit2}-*nitR*, 8789 bp	This work
pML2025	ColE1 origin, *hyg*, oriM, p_{nit1}-*cpnT*-HA- *mycgfp2*, p_{nit2}-*nitR*, 9491 bp	This work
pML2031	ColE1 origin, *hyg*, oriM, p_{nit1}-*cpnT*-HA-His, p_{nit2}-*nitR*, 9078 bp	This work
pML2040	ColE1 origin, *hyg*, oriM, p_{nit1}-*cpnT*$_{aa1-448}$-HA-His, p_{nit2}-*nitR*, 7884 bp	This work
pML2046	pBR322 origin, L5 *attP*, FRT-*hyg-int*-p_{imyc}-*cpnT*$_{aa1-448}$-FRT, 7360 bp	This work
pML2084	pBR322 origin, L5 *attP*, FRT-*hyg-int*-p_{imyc}-*esxEF-rv3902c* transcriptional fusion-FRT, 7230 bp	This work
pML2087	pBR322 origin, *aph*, L5 *attP*, FRT-*int*-p_{imyc}-*rv3902c*-FRT, 6654 bp	This work
pML2093	CMV promoter-*cpnT*$_{aa650-847}$, SV40 origin, pBR322 origin, *bla*, 5337 bp	This work
pML2123	ColE1 origin, *hyg*, oriM, p_{smyc}-*cpnT*$_{aa650-847}$ mutants (G752V, A811E, G818V) translationally fused to HA-*mycgfp2*, 6861 bp	This work
pML2138	CMV promoter-*cpnT*$_{aa650-847}$ G818V mutant, SV40 origin, pBR322 origin,*bla*, 5337 bp	This work

pML2172	ColE1 origin, *hyg*, oriM, p_{nit1}-*cpnT*$_{G818V}$-HA-His, p_{nit2}-*nitR*, 9078 bp	This work
pML2228	pBR322 origin,L5 *attP*, FRT-*hyg*-*int*-p_{imyc}-*cpnT*-FRT, 8557 bp	This work
pML2904	ColE1 origin, *aph*, oriM, p_{nit1}-*cpnT*$_{aa1-448}$-HA-His, *esxEF-rv3902c* transcriptional fusion, p_{nit2}-*nitR*, 7884 bp	This work
pML3009	PBR322 origin, *aph,* L5 *attP*, FRT-*int*-p_{imyc}-*esxF-esxE-cpnT-rv3902c*-FRT, 9790 bp	This work
pML3107	PBR322 origin, *aph,* L5 *attP*, FRT-*int*-p_{imyc}-*esxF-esxE-cpnT*$_{NTD}$-HA-His-*rv3902c*-FRT, 8656 bp	This work
pRK7	CMV promoter, SV40 origin, pBR322 origin,*bla*, 4708 bp	Addgene plasmid 10883
pWHE655-revCasp-3	pBR322 origin, *bla*, 2x 250 bp cHS4 insulators, TRE-Tight, *revCasp-3*, 2x 250 bp cHS4 insulators, mPGK promoter, $G418^R$, 7531 bp	(20)
pWHE655-CpnT$_{CTD}$	pBR322 origin, *bla*, 2x 250 bp cHS4 insulators, TRE-Tight, *cpnT*$_{CTD}$, 2x 250 bp cHS4 insulators, mPGK promoter, $G418^R$, 7354 bp	This work

Table S1: Plasmids used in this work. Up- and downstream homologous sequences of genes are subscripted as up_*gene*_hom and down_*gene*_hom. “Origin” means origin of replication. The genes *bla, hyg* and *aph* confer resistance to ampicillin, hygromycin and kanamycin, respectively. The *attP L5* site is required for site specific integration of plasmids into the chromosomal *attB* site by the mycobacteriophage L5 integrase gene, *int*. The site-specific recombinase Cre excises DNA fragments that are flanked by *loxP* recognition sites. pAL5000ts denotes the temperature-sensitive origin of replication of the pAL5000 plasmid. The constitutive mycobacterial promoters p_{smyc} and p_{imyc} have been described previously. The *sacB* gene of *B. subtilis* encodes the counterselective marker levansucrase that mediates sensitivity to sucrose. Its expression is regulated by *sacR*.

Oligonucleotide	Sequence (5'→3')
CN1390	CGACAAAGCTACGTGCGGCG
CN1393	CGCATATGGCGCCGTTGGCGGTCGATCCCGC
CN1394	CGAAGCTTCTACTGTCGCAACACCCCGCGC
CN1396	CGATTTAAATCCGCACCCGCAGCCACCAC
CN1397	CGATGCATCAACTGACCAGCACCGTTATC
CN1398	CGACTAGTCCTGGATCTCGACGGCGACG
CN1399	CGTTAATTAAGATCATCAGAACGAGATGCG
CN1537	GCTTAATTAACAGAAAGGAGGATTTCAACTATCATGGCGCCGTTGGCGGTCGATCCCGC
CN1584	CGAAGCTTCTAACCCTTATAGTCCTTCCAAAG
CN1585	GCTTAATTAACAGAAAGGAGGATTTCAACTATCGTGACAATAGGTGTGGACCTGTC
CN1644	GTCCGTACCTCCGTTGCTTG
CN1718	CTGACGCTCAGTGGAACGAAAAC
CN1720	CGGATATCCGGTGTCGTCGGCTCAAGC
CN1729	GCTTGAGCCGACGACACCGAAGCTTCG
CN1807-1907	CGGAATTCTCAGTGGTGGTGGTGGTGGTGAGTACTGGCGTAGTCCGGCACGTCGTACGGGTA CTGGCGCAGCACGCCG
CN1824	AGTACT*GGCGTAGTCCGGCACGTCGTACGGGTA*GATATCCTGTCGCAACACCCCGCGC
CN1825	TAAAGCTTTA**GTGGTGGTGGTGGTGGTG**AGTACTGGCGTAGTCCGGCAC
CN1904	CGGTCGACCATGGCAGGTGCAGTGTTTGG
CN1922	AAAGGGAGTCCATATGCGTCTGAGCGATGAAGCCGTGGAT
CN1982	CGTTAATTAAAGAAAGGAGGTTAATATGCGGTTATCCGACGAAGCGGTTGAC
CN1994	GGGTTGTGGTCAGCCGGTTGGCAGTATTCAAGTGC
CN2239	ATGAAAATC**CATCACCATCACCATCAC**GAAGAAGGTAAACTGGTAAT
CN2240	CACGAGCAATTGACCAACAAGGACCATAGATTATGAAAATCCATCAC
CN2241	CGGGTTCGGCAGCAGATCTTTGTTATAAATCAGCGATA
CN2542	GCTTAATTAACAGAAAGGAGGTAATTAATTACCATGGCGCCGTTGGCGGTCG
CN2811	TATGGCTCTGAAAATACAGGTTTTCCCCGAGGTTGTTGTTATTGTTATTGTTGTTGTTGTTC GAGCT
CN2812	CGAACAACAACAACAATAACAATAACAACAACCTCGGGGAAAACCTGTATTTTCAGAGCCA
CN2817	TTTATTTGAAGCTTTTACTGGCGCAGCACGCCGCGACGAAT
CN2932	GCTTAATTAAGGGAGAACATGGGTGCCGACGACACGCTG
CN2933	CAATTAATTAGCTAAAGCTTCTAACCCTTATAGTCCTTCC
CN2934	CCACGAATTTGGGTATGTGGTCGTGACAATAGGTGTGGACCTGTCAAC
CN2935	GTTGACAGGTCCACACCTATTGTCACGACCACATACCCAAATTCGTGG
CN3042	CGATTAATTAACAGAAAGGAGGATTTCAACTATCATGGGTGCCGACGACACGCTG
CN3047	TTGACAGGTCCACACCTATTGTCACTAGTGGTGGTGGTGGTGGTG
CN3048	GTGACAATAGGTGTGGACCTGTCAACG
CN5010	TACCCGTACGACGTGCCGGACTACGCCAGTACTTCGAAGGGCGAGGAGCTG
CN5011	GAAAAGCTTATTTAAATCTACTTGTACAGCTCGTCCATG
CN5012	GTGCGGCCAGCCGGTCGGATCCATCCAAGTGCGGA
CN5013	TCCGCACTTGGATGGATCCGACCGGCTGGCCGCAC
D3fwd-	ACTGTCGAATTCCCTCGGTTCTAAGCTTCTGC
D3rev-shEcoRV	TACAGTGATATCTCAGGCGTAGTCCGGC

Table S2: Oligonucleotides used in this work. Restriction sites are underlined. The sequence shown in italics is the sequence of the HA tag. The sequence shown in bold is the sequence of the hexahistidine tag.

Strain	Parent strain and relevant genotype	Source or reference
E. coli DH5α	*recA1; endA1; gyrA96; thi; relA1; hsdR17(rK-;mK+); supE44; ϕ80ΔlacZΔM15; ΔlacZYA-argF; UE169*	(27)
E. coli C43(DE3)	F–; *ompT; hsdSB; (rB- mB-); gal; dcm;* (DE3)	(28)
M. smegmatis mc^2155	wild-type	(29)
M. smegmatis SMR5	*M. smegmatis* mc^2155; Sm^r	(30)
M. smegmatis ML16	*M. smegmatis* SMR5; Δ*mspA* Δ*mspC* Δ*mspD*	(25)
M. smegmatis ML1910	ML16 derivative, *ΔmspAΔmspBΔmspCΔmspD, groEL1::bxb1;* L5:P_{NIT}-*cpnT*$_{NTD\text{-}HA\text{-}His}$*:* ,$Kan^R$ Hyg^R	M. Pavlenok
M. bovis BCG	strain Institute Pasteur	American Type Culture Collection (ATCC 27291)
M. bovis BCG ML1012	*M. bovis* BCG derivative, *rv3903c::IS1096,* Kan^R	(31)
M. bovis BCG ML383	*M. bovis* BCG derivative, L5::pML2008, Hyg^R	this study
M. bovis BCG ML386	ML1012 derivative, L5::pML2008, Kan^R Hyg^R	this study
M. bovis BCG ML387	ML1012 derivative, L5::pML2009, Kan^R Hyg^R	this study
M. bovis BCG ML388	ML1012 derivative, L5::pML2010, Kan^R Hyg^R	this study
M. tuberculosis H37Rv	Wild-type	American Type Culture Collection (ATCC 25618)
M. tuberculosis mc^26206	H37Rv derivative, Δ*leuCD* and Δ*panCD*	(1)
M. tuberculosis ML812	H37Rv derivative, L5::pML2008, Hyg^R	this study
M. tuberculosis ML829	H37Rv derivative, *ΔcpnT::mycgfp2+,* Hyg^R, marked mutant of *cpnT*	this study
M. tuberculosis ML845	ML829 derivative, unmarked mutant of *cpnT*	this study
M. tuberculosis ML1501	ML845 derivative. L5::pML2023, Hyg^R	this study
M. tuberculosis ML1504	ML845 derivative, L5::pML2008, Hyg^R	this study
M. tuberculosis ML1518	ML845 derivative, L5::pML2046, Hyg^R	this study
M. tuberculosis ML1528	Wild-type derivative, L5::pCV125; Kan^R	this study
M. tuberculosis ML1543	ML845 derivative, L5::pML2228, Hyg^R	this study
M. tuberculosis ML2000	ML845 derivative, L5::pCV125, Kan^R	this study
M. tuberculosis ML2001	ML845 derivative, L5::pML3009, Kan^R	this study
M. tuberculosis ML2002	ML845 derivative, L5::pML3107, Kan^R	this study
M. tuberculosis ML2003	mc^26206 derivative, *ΔcpnT::mycgfp2+,* Hyg^R, marked mutant of *cpnT*	this study
M. tuberculosis ML2004	ML2003 derivative, unmarked mutant of *cpnT*	this study
M. tuberculosis ML2010	mc^26206 derivative, L5::pML2084, Hyg^R	this study

Table S3: Strains used in this work. The annotation Hyg^R indicates that the strain is resistant to the hygromycin, Kan^R indicates that the strain is resistant to the kanamycin.

Name	Short name	Target	Conc.	Solvent	Reference	Supplier
Benzyloxycarbonyl-L-Aspart-1-yl-[(2,6-Dichlorobenzoyl) oxy]methane	Z-Asp-CH2-DCB	panCaspase	100 µM	Methanol	(32, 33)	Peptanova
N-acetyl-L-tyrosyl-L-valyl-N-[(1S)-1-(carboxymethyl)-3-chloro-2-oxopropyl]	Ac-YVAD-CMK	Caspase-1	40 µM	DMSO	(34)	Peptanova
Cyclo-(L-Alanyl-D-alanyl-N-methyl-L-leucyl-N-methyl-L-leucyl-N-methyl-L-valyl-3-hydroxy-N,4-dimethyl-L-2-amino-6-octenoyl-L-a-amino-butyryl-N-methylglycyl-N-methyl-L-leucyl-L-valyl-N-methyl-L-leucyl)	Cyclo-sporin A	Cyclophilin D	5 µM	DMSO	(35)	Sigma
5-(1H-Indol-3-ylmethyl)-3-methyl-2-thioxo-4-Imidazolidinone	Necro-statin-1	Ripk1	30 µM	DMSO	(36, 37)	Sigma
butylated hydroxyansisol	BHA	antioxidant	100 µM	Ethanol	-	Sigma

Table S4: Cell death inhibitors used in this study. Chemical designations, commonly used names, molecular targets, concentrations used in this study, the respective solvents, literature references and the supplier are listed for all inhibitors tested in this study.

SUPPLEMENTARY REFERENCES

1. Sampson SL*, et al.* (2004) Protection elicited by a double leucine and pantothenate auxotroph of *Mycobacterium tuberculosis* in guinea pigs. *Infect Immun* 72(5):3031-3037.
2. Smeulders MJ, Keer J, Speight RA, & Williams HD (1999) Adaptation of *Mycobacterium smegmatis* to stationary phase. *J. Bacteriol.* 181(1):270-283.
3. Wolschendorf F, Mahfoud M, & Niederweis M (2007) Porins are required for uptake of phosphates by *Mycobacterium smegmatis*. *J Bacteriol* 189(6):2435-2442.
4. Mailaender C*, et al.* (2004) The MspA porin promotes growth and increases antibiotic susceptibility of both *Mycobacterium bovis* BCG and *Mycobacterium tuberculosis*. *Microbiology* 150(Pt 4):853-864.
5. Pandey AK*, et al.* (2009) Nitrile-inducible gene expression in mycobacteria. *Tuberculosis (Edinb)* 89(1):12-16.
6. Kaps I*, et al.* (2001) Energy transfer between fluorescent proteins using a co-expression system in *Mycobacterium smegmatis*. *Gene* 278(1-2):115-124.
7. Domenech P & Reed MB (2009) Rapid and spontaneous loss of phthiocerol dimycocerosate (PDIM) from *Mycobacterium tuberculosis* grown in vitro: implications for virulence studies. *Microbiology* 155(Pt 11):3532-3543.
8. Kirksey MA*, et al.* (2011) Spontaneous phthiocerol dimycocerosate-deficient variants of *Mycobacterium tuberculosis* are susceptible to gamma interferon-mediated immunity. *Infect Immun* 79(7):2829-2838.
9. Danilchanka O, Pavlenok M, & Niederweis M (2008) Role of porins for uptake of antibiotics by *Mycobacterium smegmatis*. *Antimicrob Agents Chemother* 52(9):3127-3134.
10. Wells RM*, et al.* (2013) Discovery of a siderophore export system essential for virulence of *Mycobacterium tuberculosis*. *PLoS Pathog* 9(1):e1003120.
11. Ojha A*, et al.* (2005) GroEL1: a dedicated chaperone involved in mycolic acid biosynthesis during biofilm formation in mycobacteria. *Cell* 123(5):861-873.
12. Heinz C & Niederweis M (2000) Selective extraction and purification of a mycobacterial outer membrane protein. *Anal. Biochem.* 285(1):113-120.
13. Angelova MI (2001) Giant Vesicles. *Liposome electroformation*, ed P.L. Luisi PW (John Wiley and Sons Ltd, Chichester), pp 27-36.
14. Kreir M, Farre C, Beckler M, George M, & Fertig N (2008) Rapid screening of membrane protein activity: electrophysiological analysis of OmpF reconstituted in proteoliposomes. *Lab Chip* 8(4):587-595.
15. Bruggemann A*, et al.* (2008) Planar patch clamp: advances in electrophysiology. *Methods Mol Biol* 491:165-176.
16. Farre C*, et al.* (2007) Automated ion channel screening: patch clamping made easy. *Expert Opin Ther Targets* 11(4):557-565.
17. Siroy A*, et al.* (2008) Rv1698 of *Mycobacterium tuberculosis* represents a new class of channel-forming outer membrane proteins. *J. Biol. Chem.* 283(26):17827-17837.
18. Kapust RB*, et al.* (2001) Tobacco etch virus protease: mechanism of autolysis and rational design of stable mutants with wild-type catalytic proficiency. *Protein Eng* 14(12):993-1000.
19. Srinivasula SM*, et al.* (1998) Generation of constitutively active recombinant caspases-3 and -6 by rearrangement of their subunits. *J Biol Chem* 273(17):10107-10111.
20. Danke C*, et al.* (2010) Adjusting transgene expression levels in lymphocytes with a set of inducible promoters. *J Gene Med* 12(6):501-515.
21. Herr R, Wohrle FU, Danke C, Berens C, & Brummer T (2011) A novel MCF-10A line allowing conditional oncogene expression in 3D culture. *Cell Commun Signal* 9:17.

22. Munoz LE*, et al.* (2013) Colourful death: Six-parameter classification of cell death by flow cytometry-Dead cells tell tales. *Autoimmunity* 46(5):336-341.
23. Nicoletti I, Migliorati G, Pagliacci MC, Grignani F, & Riccardi C (1991) A rapid and simple method for measuring thymocyte apoptosis by propidium iodide staining and flow cytometry. *J Immunol Methods* 139(2):271-279.
24. Alland D, Steyn AJ, Weisbrod T, Aldrich K, & Jacobs WR, Jr. (2000) Characterization of the *Mycobacterium tuberculosis iniBAC* promoter, a promoter that responds to cell wall biosynthesis inhibition. *J. Bacteriol.* 182(7):1802-1811.
25. Stephan J*, et al.* (2005) The growth rate of *Mycobacterium smegmatis* depends on sufficient porin-mediated influx of nutrients. *Mol. Microbiol.* 58(3):714-730.
26. Wolschendorf F*, et al.* (2011) Copper resistance is essential for virulence of *Mycobacterium tuberculosis*. *Proc Natl Acad Sci U S A* 108(4):1621-1626.
27. Sambrook J, Fritsch EF, & Maniatis T (1989) *Molecular cloning: a laboratory manual* (Cold Spring Harbor Laboratory Press, Cold Spring Harbor, N. Y.) 2nd Ed.
28. Miroux B & Walker JE (1996) Over-production of proteins in *Escherichia coli*: mutant hosts that allow synthesis of some membrane proteins and globular proteins at high levels. *J Mol Biol* 260(3):289-298.
29. Snapper SB, Melton RE, Mustafa S, Kieser T, & Jacobs WR, Jr. (1990) Isolation and characterization of efficient plasmid transformation mutants of *Mycobacterium smegmatis*. *Mol Microbiol* 4(11):1911-1919.
30. Sander P, Meier A, & Boettger EC (1995) *rpsL*+: a dominant selectable marker for gene replacement in mycobacteria. *Mol. Microbiol.* 16(5):991-1000.
31. Danilchanka O, Mailaender C, & Niederweis M (2008) Identification of a novel multidrug efflux pump of *Mycobacterium tuberculosis*. *Antimicrob Agents Chemother* 52(7):2503-2511.
32. Fujino M, Li XK, Guo L, Amano T, & Suzuki S (2001) Activation of caspases and mitochondria in FTY720-mediated apoptosis in human T cell line Jurkat. *Int Immunopharmacol* 1(11):2011-2021.
33. Kato M, Nonaka T, Maki M, Kikuchi H, & Imajoh-Ohmi S (2000) Caspases cleave the amino-terminal calpain inhibitory unit of calpastatin during apoptosis in human Jurkat T cells. *J Biochem* 127(2):297-305.
34. Rupper AC & Cardelli JA (2008) Induction of guanylate binding protein 5 by gamma interferon increases susceptibility to Salmonella enterica serovar Typhimurium-induced pyroptosis in RAW 264.7 cells. *Infect Immun* 76(6):2304-2315.
35. Lee J, Repasy T, Papavinasasundaram K, Sassetti C, & Kornfeld H (2011) *Mycobacterium tuberculosis* induces an atypical cell death mode to escape from infected macrophages. *PLoS One* 6(3):e18367.
36. Ch'en IL, Tsau JS, Molkentin JD, Komatsu M, & Hedrick SM (2011) Mechanisms of necroptosis in T cells. *J Exp Med* 208(4):633-641.
37. Degterev A*, et al.* (2005) Chemical inhibitor of nonapoptotic cell death with therapeutic potential for ischemic brain injury. *Nat Chem Biol* 1(2):112-119.